

SKIP-IT? THEORETICAL CONDITIONS FOR LAYER SKIPPING IN VISION–LANGUAGE MODELS

Max Hartman*

Department of Electrical & Computer Engineering
University of Illinois Urbana-Champaign
maxh3@illinois.edu

Vidhata Jayaraman*

Department of Electrical & Computer Engineering
Department of Mathematics
University of Illinois Urbana-Champaign
vidhata2@illinois.edu

Moulik Choraria

Department of Electrical & Computer Engineering
University of Illinois Urbana-Champaign
moulikc2@illinois.edu

Akhil Bhimaraju

Department of Electrical & Computer Engineering
University of Illinois Urbana-Champaign
akhilb3@illinois.edu

Lav R. Varshney

AI Innovation Institute
Stony Brook University
lav.varshney@stonybrook.edu

ABSTRACT

Vision–language models (VLMs) achieve incredible performance across a wide range of tasks, but their large size makes inference costly. Recent work shows that selectively skipping VLM layers can improve efficiency with minimal performance loss or even performance improvements. However, this technique remains underused due to the limited understanding of when layer skipping is beneficial. In this paper, we develop a framework that uses information and learning theory to characterize the conditions under which layer skipping enhances efficiency without sacrificing performance. Motivated by these observations, we analyze the evolution of the VLM’s hidden representations through the LLM backbone and show that layers with large redundancy as predicted by our framework coincide with those skipped by popular layer-skipping methods in practice, providing a unified theoretical scaffolding for multiple efficient inference techniques. Our experiments demonstrate that skipping such layers yields faster inference that preserves performance, and also show that applying skipping outside these conditions leads to model degradation.

1 INTRODUCTION

Vision–language models (VLMs) such as BLIP (Li et al., 2022), LLaVA (Liu et al., 2023; 2024a), and more recently, Qwen (Bai et al., 2023; Qwen et al., 2025), and Deepseek-VL (Lu et al., 2024) have become more popular over the past few years due to their impressive performance. Nevertheless, these models come with escalating training and inference costs (Jin et al., 2024), creating barriers to widespread adoption. This computational burden stems from the fact that these models typically build upon large language model backbones, requiring the processing of extensive sequences of image tokens alongside text, particularly when handling high-resolution images.

In response to these challenges, techniques to improve VLM efficiency have grown in popularity, aiming to reduce model overhead while maintaining performance. Many approaches build upon efficiency methods from large language models (LLMs), broadly classified as training time or inference time improvements. Training time methods include parameter-efficient approaches such as LoRA (Hu et al., 2022; Dettmers et al., 2023; Biderman et al., 2024) and Mixture of Experts (MoE)

*Equal contribution

(Artetxe et al., 2022; Bao et al., 2022; Lin et al., 2024), while inference time methods encompass token compression, skipping, and quantization. Token compression techniques (Chen et al., 2024a; Vasu et al., 2025; Liu et al., 2025) reduce redundancy in vision representations, while layer skipping, initially developed for efficient LLM inference (Elhoushi et al., 2024), eliminates processing redundancy during forward passes. This work focuses on layer skipping techniques for VLM efficiency. Recent VLM-specific methods include AdaSkip (He et al., 2025), FlexiDepth (Luo et al., 2025a), and retrained models like DeepInsert (Choraria et al., 2025), MoLe-VLA (Zhang et al., 2025), and γ -MoD (Luo et al., 2025b). Despite their empirical success, their identification of layers to skip is ad hoc and lacks principled justification.

In this work, we propose a learning- and information-theoretic framework to formulate an experimentally easy-to-compute condition that indicates when there are redundant text and/or vision tokens that can be skipped to improve efficiency without degrading performance. We validate our framework first by experimentally verifying the existence of *Functional Redundancy* and *Informational Redundancy*. We then use these results to predict which layers and tokens can be skipped at the beginning (late entry) and end (early exit) of a set of models. Inversely, we further show that model performance degrades when our conditions are not met.

Overall, our contributions are as follows.

1. We propose a theoretical framework to study redundancies across layers. These redundancies can be used with cross-attention analysis to improve inference-time efficiency.
2. We experimentally verify that the necessary conditions from theory are met in the early and late vision tokens across all models. We consider the average cosine distance and the probability of a small cosine distance between adjacent layers.
3. We run layer skipping experiments to validate that fulfilling the redundancy and cross-attention conditions corresponds to improved model efficiency with minimal performance degradation, whereas not meeting them leads to performance degradation.

2 RELATED WORK

2.1 VISION LANGUAGE MODELS

VLMs feed vision and textual tokens into an autoregressive LLM. BLIP models (Li et al., 2022; 2023) were some of the first to introduce vision-language pretraining, with the latter using a Q-former to connect frozen image encoders with LLMs. Flamingo introduced the ability to ingest mixed insertions of images, videos, and text (Alayrac et al., 2022). LLaVA introduced a multimodal instruction-following model. LLaVA-NeXT built on LLaVA with improved reasoning and performance (Liu et al., 2024a). More recently, Molmo improved capabilities in pointing and counting tasks (Deitke et al., 2025). LLaMA-4 introduced a mixture-of-experts VLM with a massive context length. Specifically, LLaMA-4 Scout has a token context length of 10M (Meta AI, 2024). In most models, the vision tokens are obtained from a pretrained vision encoder, such as CLIP (Radford et al., 2021) or SigLIP (Zhai et al., 2023). Some core challenges in these models include inference-time inefficiency, multimodal alignment, and vision interpretability.

2.2 LAYER SKIPPING

Redundancies in tokens and layers have motivated efficiency techniques in both LLMs and VLMs. In LLMs, AdaSkip introduces sublayer-wise skipping for long-context inference (He et al., 2025), while FlexiDepth enables adaptive layer skipping (Luo et al., 2025a). Both exploit redundancy to reduce computation while maintaining performance. Multimodal models have adopted similar strategies: γ -MoD converts dense layers into sparse Mixture-of-Depth layers (Luo et al., 2025b), MoLe-VLA applies layer skipping to robot manipulation (Zhang et al., 2025), and DeepInsert injects vision tokens at later layers to reduce early-layer overhead (Choraria et al., 2025). Parallel work focuses on token reduction through multimodal skipping or early exit. FastV prunes visual tokens by learning attention patterns (Chen et al., 2024a), Visual Token Withdrawal (VTW) removes visual tokens after certain layers (Lin et al., 2025), and PruMerge leverages visual encoder sparsity to discard tokens (Shang et al., 2025). Our work establishes a principled framework to understand when layer-skipping is feasible.

2.3 VLM INTERPRETABILITY

VLM interpretability focuses on understanding vision–language models, a space that remains less explored than LLM interpretability. Two notable VLM-specific methods are *logit lens* and *causal tracing* (Neo et al., 2025; Jiang et al., 2025; Basu et al., 2024). The *logit lens* uses the unembedding matrix to reveal textual representations of visual tokens and localize visually grounded factual information. *Causal tracing* identifies which layers carry visual knowledge by perturbing prompts to remove image dependence and then copying activations from the unperturbed forward pass. Both techniques adapt earlier LLM interpretability methods: the *logit lens* from Nostalgebraist (2020) and causal tracing from Meng et al. (2023; 2022). Our work also has clear applications to VLM interpretability. The definitions and theorems we propose for measuring redundancies between layers can help determine the functionality of specific layers and give guidance on how information is propagated through the model.

3 FRAMEWORK

In this section, we provide a framework to analyze token copying and redundancy in VLMs. We first define our notions of redundancy and then connect experimentally-verifiable notions of redundancy to stronger, more informative notions of redundancy. These results help isolate locations where a specific modality (vision or language) is being copied across layers. Then, by combining with additional metrics for quantifying inter-modality interaction via cross-attention, we determine layers viable for skipping. Note that for general skipping of layers, both high levels of redundancy and small cross-attention are necessary conditions. If one only has high amounts of redundancy, the two modalities may still be communicating with each other, so the entire removal of one modality is not viable. Conversely, if one only has small cross-attention, the representations may still be evolving across the layers for each modality independently, which can cascade errors deeper in the model, and so skipping is, again, not viable.

To formally define layer skipping, consider a VLM with n layers, ϕ_θ^n . Let $X = \begin{pmatrix} X_{text} \\ X_{vis} \end{pmatrix}$ be the input to the VLM. We consider late entry, say of the vision tokens, in the first ℓ layers to be $\phi_\theta^{n-\ell}(\begin{pmatrix} \phi_\theta^\ell(X_{text}) \\ X_{vis} \end{pmatrix})$. A visual of this layer skipping can be seen in Figure 1.

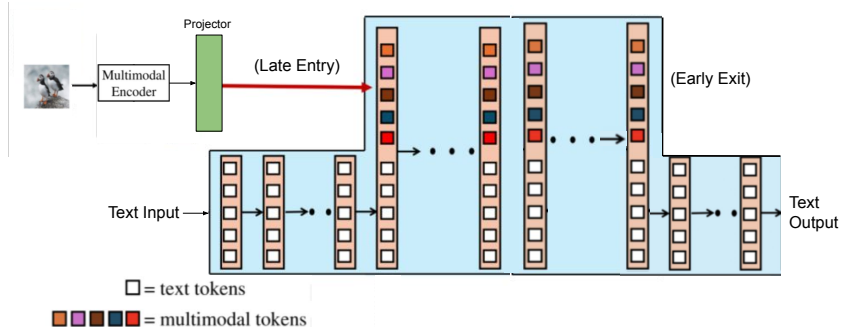


Figure 1: Early Exit and Late Entry. Specifically, the visual tokens are not passed into the first few layers but instead, directly inserted along with the prompt to the chosen layer for insertion or the vision tokens are removed from the forward pass after a certain layer.

We observe from Figure 1 that late entry of vision tokens requires redundancy in the early visual layers. This redundancy ensures that simply inserting the original image tokens remains viable, while small cross-attention is necessary since the text tokens cannot depend heavily on information from the visual tokens. In contrast, for early exit of vision tokens, a small cross-attention is already sufficient: even if the vision tokens continue to evolve, their limited influence on the text tokens makes it viable to skip them.

3.1 DEFINITIONS OF REDUNDANCY

Redundancy, in this setting, quantifies how little the current hidden state has changed relative to the previous one. A simple and accessible way to capture redundancy between layers is to measure the similarity of hidden states using an average (cosine) distance. We refer to this as geometric redundancy.

Definition 1 (Geometric ϵ -redundancy). *Let $\rho : \mathcal{X} \times \mathcal{X} \rightarrow [0, \infty)$ be a symmetric function (e.g. cosine distance or a metric). Then given random variables $X_{\ell-1}, X_\ell$ and $\epsilon > 0$, geometric ϵ -redundancy (or geometric redundancy) is $\mathbb{E}[\rho(X_{\ell-1}, X_\ell)] < \epsilon$.*

We similarly define proximal redundancy as being when layers are close together with high probability.

Definition 2 (t -proximal with probability $1 - \epsilon$; Proximal Redundancy). *Let $\rho : \mathcal{X} \times \mathcal{X} \rightarrow [0, \infty)$ be a symmetric function (e.g. cosine distance or a metric), t be some threshold value, and $\epsilon > 0$. Then random variables $X_{\ell-1}, X_\ell$ are t -proximal with probability $1 - \epsilon$ (or proximally redundant) if $\mathbb{P}[\rho(X_\ell, X_{\ell-1}) < t] > 1 - \epsilon$.*

While geometric and proximal redundancy capture semantic similarity, they do not offer much operational meaning or describe the actual redundancy between layers. To rigorously define redundancy between layers, we propose these additional notions of redundancy.

Definition 3 (Functional ϵ -redundancy). *Given a task variable Z , two random variables $X_{\ell-1}, X_\ell$, and $\epsilon > 0$, functional ϵ -redundancy (functional redundancy) is $\mathbb{E}[\|E[Z|X_\ell] - \mathbb{E}[Z|X_{\ell-1}]\|_2^2] < \epsilon$.*

Definition 4 (Informational ϵ -redundancy). *Given random variables $X_{\ell-1}, X_\ell$ and $\epsilon > 0$, informational ϵ -redundancy (informational redundancy) is $H(X_\ell|X_{\ell-1}) < \epsilon$.*

The remainder of this section connects these four notions. Specifically, we show that geometric and proximal redundancy, although less informative definitions, imply more operational forms of redundancy under natural assumptions.

3.2 FUNCTIONAL REDUNDANCY

We begin by analyzing functional redundancy, which measures the difference between optimal estimators on a task Z .

Theorem 1. *Let $X_\ell, X_{\ell-1}$ be unit-norm random variables and Z be the random variable of predictive interest (e.g. normalized hidden representations of layers $\ell, \ell - 1$ and the task ground truth respectively). Let $\rho(x, y) = 1 - \frac{\langle x, y \rangle}{\|x\|\|y\|}$. Assume $\mathbb{E}[\rho(X, Y)] < \frac{\epsilon}{2}$ and that*

$$h(x, y) = E[Z|X_\ell = x, X_{\ell-1} = y]$$

is α -Lipschitz in the first argument and β -Lipschitz in the second. Then $\mathbb{E}[\|E[Z|X_\ell] - E[Z|X_{\ell-1}]\|_2^2] < 2(\alpha^2 + \beta^2)\epsilon$.

Proof. We prove this by first translating the cosine distance into mean squared error and then using the optimality of the conditional mean and the tower property. For more details, see Appendix A.2. \square

In words, Theorem 1 establishes that under some regularity assumptions, there is a bridge between geometric redundancy and functional redundancy. However, in practice, we can never achieve these optimal estimators, so Theorem 2 bounds empirical estimates of these optimal estimators.

Theorem 2. *Let $X_\ell, X_{\ell-1}$ be unit-norm random variables and Z be the random variable of predictive interest, as before. Let $\rho(x, y) = 1 - \frac{\langle x, y \rangle}{\|x\|\|y\|}$. Assume $\mathbb{E}[\rho(X, Y)] < \frac{\epsilon}{2}$ and that*

$$h(x, y) = E[Z|X_\ell = x, X_{\ell-1} = y]$$

is α -Lipschitz in the first argument and β -Lipschitz in the second. Let \hat{f}_ℓ be a finite-sample estimate of $f_\ell^(x) = \mathbb{E}[Z|X_\ell = x]$ and $\hat{f}_{\ell-1}(x)$ be a finite-sample estimate of $f_{\ell-1}^*(x) = \mathbb{E}[Z|X_{\ell-1} = x]$. Further let, $\eta_\ell = \mathbb{E}[\|\hat{f}_\ell(X_\ell) - f_\ell^*(X_\ell)\|^2]$ and $\eta_{\ell-1} = \mathbb{E}[\|\hat{f}_{\ell-1}(X_{\ell-1}) - f_{\ell-1}^*(X_{\ell-1})\|^2]$. Then:*

$$\mathbb{E}[\|\hat{f}_\ell(X_\ell) - \hat{f}_{\ell-1}(X_{\ell-1})\|^2] < 3\eta_\ell + 3\eta_{\ell-1} + 6(\alpha^2 + \beta^2)\epsilon.$$

Proof. We prove this by again converting from cosine distance to mean squared error and then rewriting $\hat{f}_\ell(X_\ell) - \hat{f}_{\ell-1}(X_{\ell-1})$ as $(\hat{f}_\ell(X_\ell) - f_\ell^*(X_\ell)) + (f_{\ell-1}^*(X_{\ell-1}) - \hat{f}_{\ell-1}(X_{\ell-1})) + (f_\ell^*(X_\ell) - f_{\ell-1}^*(X_{\ell-1}))$. We then upper bound $\hat{f}_\ell(X_\ell) - \hat{f}_{\ell-1}(X_{\ell-1})$ using this new form by invoking Theorem 1 along with the definitions of η_ℓ and $\eta_{\ell-1}$. For more details, refer to Appendix A.2 \square

Thus, under the same regularity assumptions, we obtain guarantees for empirical estimators that mirror those for optimal ones. Importantly, the bound still decays linearly in ϵ , showing that empirical functional redundancy inherits the same behavior.

3.3 INFORMATIONAL REDUNDANCY

We now turn to informational redundancy, which asks whether the output of one layer can be (nearly) determined from the output of the previous one. This is formalized via the conditional entropy $H(X_\ell|X_{\ell-1})$.

We first get an upper bound on $H(X_\ell|X_{\ell-1})$ from Duchi & Wainwright (2013). If this upper bound is sufficiently low, this shows a high statistical correlation between X_ℓ and $X_{\ell-1}$. In other words, there is a large amount of redundancy between X_ℓ and $X_{\ell-1}$. We then use a complementary lower bound from Braun & Pokutta (2015) on the mutual information $I(X_\ell; X_{\ell-1})$. If this lower bound is sufficiently large, we can then show that there is a large amount of information shared between the two layers, thereby also implying a large amount of redundancy.

To understand these bounds, first define $P_t = \mathbb{P}[\rho(X_\ell, X_{\ell-1}) > t]$ where ρ is some symmetric function (e.g. cosine distance or a metric). P_t is the probability that the “distance” between the two random variables is greater than t . Duchi & Wainwright (2013) provide an upper bound on $H(X_\ell|X_{\ell-1})$ with respect to P_t while Braun & Pokutta (2015) give a complementary lower bound on $I(X_\ell; X_{\ell-1})$ with respect to P_t without any of the distributional assumptions that Duchi & Wainwright (2013) make. Refer to Theorems 3 and 4 in Appendix A.2 for more details on these bounds.

There is substantial prior work, such as Xu et al. (2020); Dissanayake et al. (2025), which has shown that concepts like usable information and unique/redundant information are useful for analyzing machine learning paradigms. See Appendix E for further discussion of the connection to partial information decomposition (PID).

3.4 RELATING ALL NOTIONS OF REDUNDANCY

We now give some final results to connect all notions of redundancy.

Proposition 1. *Let $\rho : \mathcal{X} \times \mathcal{X} \rightarrow \mathbb{R}$ be a symmetric function with $0 \leq \rho \leq 1$. Then*

$$\mathbb{P}[\rho(X, Y) > t] < \frac{\epsilon - t}{1 - t} \text{ implies } \mathbb{E}[\rho(X, Y)] < \epsilon,$$

Proof. Apply the tail integration formula and split the integral into a part from 0 to t and another part from t to 1. Refer to Appendix A.2 for more details. \square

Thus, under natural assumptions, proximal redundancy implies geometric redundancy.

Theorem 5 shows that under some additional natural Markov and boundedness assumptions, informational redundancy implies functional redundancy.

Theorem 5. *Suppose there are random variables $Z, X_\ell, X_{\ell-1}$ with $Z \in \mathbb{R}^d$ and $X_\ell, X_{\ell-1}$ discrete random variables. Further suppose $\|Z\|_2 \leq B$ almost surely and that $X_{\ell-1} — X_\ell — Z$ is a Markov chain. Then $\mathbb{E}[\|\mathbb{E}[Z|X_\ell] - \mathbb{E}[Z|X_{\ell-1}]\|_2^2] \leq 2B^2 H(X_\ell|X_{\ell-1})$.*

Proof. We prove this first by expressing $\mathbb{E}[Z|X_\ell = a] - \mathbb{E}[Z|X_{\ell-1} = b] = \int_{\mathbb{R}^d} z(p_{Z|X_\ell=a}(z) - p_{Z|X_{\ell-1}=b}(z))dz$. We can then bound $\|\mathbb{E}[Z|X_\ell = a] - \mathbb{E}[Z|X_{\ell-1} = b]\|$ using the triangle inequality. We then use Pinsker’s inequality to bound $\int_{\mathbb{R}^d} |p_{Z|X_\ell=a}(z) - p_{Z|X_{\ell-1}=b}(z)|dz$ using KL-divergence. Since $X_{\ell-1} — X_\ell — Z$ is a Markov chain, we can convert this into an upper bound using conditional entropy (Lemma 4). For more details, refer to Appendix A.2. \square

This result shows that informational redundancy is a more fundamental type of redundancy as it generalizes functional redundancy. Furthermore, the connection to PID gives an interesting way to interpret this bound: under certain conditions, the average difference in performance between optimal MSE estimators based on random variables X and Y is upper bounded by unique information about X that only X has. Refer to Appendix E for more details on PID.

From these results, we have that proximal redundancy implies geometric and informational redundancy, each of which, in turn, implies functional redundancy. Figure 2 summarizes these derived results.

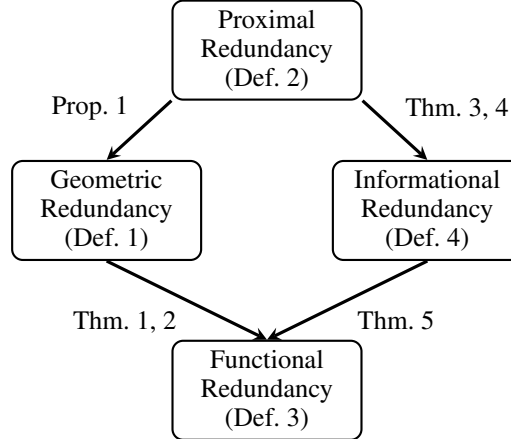


Figure 2: Implication relationships among different notions of redundancy.

4 VALIDATION OF FUNCTIONAL AND INFORMATIONAL REDUNDANCY

To find redundancies of a modality in layers, we aim to experimentally identify cases of significant geometric and proximal redundancy. Mathematically, this means that for $0 < \epsilon, t \ll 1$, $\mathbb{E}[\rho(X_\ell, X_{\ell-1})] < \epsilon$ and $\mathbb{P}[\rho(X_\ell, X_{\ell-1}) < t] > 1 - \epsilon$. From Theorems 1 and 3 we know that these conditions will imply functional and informational redundancy.

4.1 EXPERIMENTAL SETUP

In this experiment, we consider the hidden states of each token across each layer. We compute both the average cosine distance and the probability of a small average cosine distance between adjacent hidden states. We separate vision and textual tokens so that we can evaluate their differences. Formally, let H_T and H_V denote the sets of textual and visual hidden states for all layers. For token i at layer ℓ , let $h_{\ell,i}$ denote its hidden state. We define the average cosine distance between adjacent layers as

$$\mathcal{D}_\ell^{(T)} := \frac{1}{N_T} \sum_{i=1}^{N_T} \rho(h_{\ell,i}^T, h_{\ell-1,i}^T), \quad \mathcal{D}_\ell^{(V)} := \frac{1}{N_V} \sum_{i=1}^{N_V} \rho(h_{\ell,i}^V, h_{\ell-1,i}^V), \quad (1)$$

and define the probability of being close as

$$p_\ell(t; H_T) := \frac{1}{N_T} \sum_{i=1}^{N_T} \mathbb{1}\{\rho(h_{\ell,i}^T, h_{\ell-1,i}^T) < t\}, \quad p_\ell(t; H_V) := \frac{1}{N_V} \sum_{i=1}^{N_V} \mathbb{1}\{\rho(h_{\ell,i}^V, h_{\ell-1,i}^V) < t\}, \quad (2)$$

where t is a user-specified threshold, $N_T = |H_T^{(\ell)}|$ and $N_V = |H_V^{(\ell)}|$ are the number of textual and visual tokens, respectively, $h_{\ell,i}^T, h_{\ell-1,i}^T \in H_T$, $h_{\ell,i}^V, h_{\ell-1,i}^V \in H_V$, and $\rho(\cdot, \cdot)$ denotes cosine distance. This is done for $\ell \in [1, N]$, where N is the number of layers in the specific model.

4.2 MODELS & DATASETS

Both experiments use LLaVA 1.5 (7B and 13B) (Liu et al., 2023) and LLaVA NeXT (1.6) (Liu et al., 2024a) as VLMs. Additional results using DeepSeek-VL (7B base) (Lu et al., 2024) and Qwen 2.5 VL (Qwen et al., 2025) are in Appendix C.

The experiments are performed using multiple choice and free response datasets, spanning a diverse set of vision-language tasks including general question answering (GQA (Hudson & Manning, 2019), VQA (Agrawal et al., 2015), Visual7W (Zhu et al., 2016)), text, OCR, and document-based (AI2D (Kembhavi et al., 2016), OCRBench (Liu et al., 2024b), TextVQA (Singh et al., 2019)), and multimodal reasoning (MMMU (Yue et al., 2024), RealWorldQA (xAI, 2024), MMStar (Chen et al., 2024b), MathVision (Wang et al., 2024)). For further details on dataset and evaluation protocols, please refer to the Appendix B.

4.3 RESULTS

Figure 4 shows that the early layer vision tokens have very low cosine distances with each other ($\rho(X_\ell, X_{\ell-1}) < \epsilon$) and very high probability of being close to each other (0.05-proximal with probability $> 1 - \epsilon$). In the later layers of LLaVA 1.5 7B and 13B, both the early and textual tokens demonstrate proximal redundancy ($t = 0.05$, probability $\geq 1 - \epsilon$). In LLaVA 1.6, this trend is visible but not as extreme. Note that the 0.05 threshold is arbitrary; we seek to highlight that early vision tokens have low high probabilities of being close, which means that there are redundancies via Theorems 1—4. Additionally, for each model, the adjacent distances and probabilities for both vision and textual tokens across all tested datasets are similar. This indicates that the model itself is more important in determining which layers can be dropped relative to the dataset itself. Refer to Appendix C for additional results.

The results in this section indicate that these models exhibit clear redundancy that can be exploited for efficiency improvements. We now validate that the cross-attention between the modalities is sufficiently low to allow for late entry. As stated in Section 3, minimal cross-attention is sufficient for early exit.

4.4 CROSS-ATTENTION ANALYSIS

To determine layers viable for skipping, we analyze cross-attention in addition to redundancy to ensure the inter-modality interaction is minimal. If inter-modality interaction is not minimal, then even if one modality has significant redundancy, its output is still necessary for processing in the other modality, so skipping is not viable. In Figure 3 we use the Visual Attention Ratio (VAR) from Jiang et al. (2025) to visualize the cross-attention between vision and text. Specifically, they define VAR for each head h at layer ℓ for the k -th text token \mathbf{y}_k to be

$$\text{VAR}^{(\ell)}(\mathbf{y}_k) \triangleq \sum_{j=0}^h \sum_{i=1}^n \mathbf{A}_k^{(\ell,j)}(a_k, i) \quad (3)$$

where $\mathbf{A}_k^{(\ell,j)}(a_k, i)$ is the head-wise sum of the attention weights of the newly generated token \mathbf{y}_k assigned to the image token \mathbf{v}_i . We, in particular, visualize just the VAR with respect to the answer token. From the plots in Figure 3 we see that in general across all datasets and models the early and late layers have minimal cross attention according to this metric in comparison to the middle layers. Previous work has described that this happens because the majority of visual information processing happens in these layers (Lin et al., 2025; Shang et al., 2025; Choraria et al., 2025; Jiang et al., 2025).

5 IMPACT ON MODEL PERFORMANCE

In this section, we run two skipping experiments using the same setup as before to validate whether the conditions being met or not are directly related to model degradation. Based on our results above and Theorems 1—4 we deduce that the early and late layers are often highly redundant with respect to visual information. Therefore we experiment running late entry and early stopping on vision tokens. We then compare the performance of these experiments to whether or not the conditions of

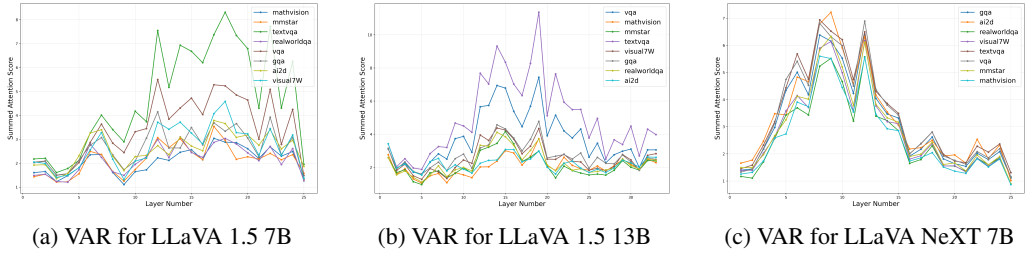


Figure 3: Visual Attention Ratio (VAR) (Jiang et al., 2025) with respect to the answer text token for the LLaVA 7B and 13B. One can see that the majority of the cross-attention is isolated to the middle layers, and the early and late layers have minimal cross-attention.

redundancy are being met. In this way, we show that the proposed conditions can be acted on to improve the efficiency of VLM.

5.1 RESULTS

The table below provides a summary of the main results of this work.

Task	Metric	LLaVA 1.5 7B			LLaVA NeXT 7B			LLaVA 1.5 13B					
		0	4	8	12	0	4	8	12	0	4	8	12
General VQA	$\rho(V_\ell, V_{\ell-1})$	–	0.025	0.073	0.060	–	0.006	0.037	0.070	–	0.025	0.066	0.058
	$\mathbb{P}[D_V < 0.05]$	–	0.972	0.267	0.271	–	0.974	0.791	0.334	–	0.965	0.273	0.403
	Accuracy	0.564	0.553	0.370	0.261	0.770	0.721	0.630	0.514	0.782	0.779	0.747	0.5010
Text/Doc VQA	$\rho(V_\ell, V_{\ell-1})$	–	0.020	0.061	0.058	–	0.007	0.039	0.037	–	0.019	0.059	0.059
	$\mathbb{P}[D_V < 0.05]$	–	0.992	0.378	0.337	–	0.967	0.891	0.410	–	0.995	0.362	0.411
	Accuracy	0.5790	0.5640	0.5130	0.4920	0.703	0.5400	0.4420	0.3320	0.6920	0.6780	0.6260	0.6000
Multimodal Reasoning (Guessing)	$\rho(V_\ell, V_{\ell-1})$	–	0.019	0.056	0.053	–	0.011	0.033	0.061	–	0.019	0.062	0.060
	$\mathbb{P}[D_V < 0.05]$	–	0.987	0.465	0.427	–	0.939	0.871	0.413	–	0.995	0.361	0.402
	Accuracy	0.255	0.250	0.242	0.228	0.231	0.143	0.105	0.088	0.261	0.256	0.253	0.195
Multimodal Reasoning (Not Guessing)	$\rho(V_\ell, V_{\ell-1})$	–	0.025	0.072	0.059	–	0.008	0.036	0.067	–	0.024	0.066	0.058
	$\mathbb{P}[D_V < 0.05]$	–	0.965	0.333	0.322	–	0.961	0.821	0.346	–	0.978	0.314	0.441
	Accuracy	0.325	0.321	0.302	0.233	0.384	0.248	0.258	0.155	0.341	0.343	0.316	0.245

Table 1: Summary of results for layer skipping on vision tokens. In this table, we only focus on the first 16 layers of each model. After this point, skipping causes each model to degrade even further.

Task	Metric	LLaVA 1.5 7B			LLaVA NeXT 7B			LLaVA 1.5 13B				
		20	24	28	20	24	28	20	24	28	32	36
General VQA	$\rho(V_\ell, V_{\ell-1})$	0.038	0.026	0.023	0.052	0.047	0.077	0.041	0.024	0.018	0.018	0.029
	$\rho(T_\ell, T_{\ell-1})$	0.028	0.016	0.017	0.046	0.032	0.056	0.042	0.021	0.012	0.012	0.019
	$\mathbb{P}[D_V < 0.05]$	0.786	0.954	0.995	0.502	0.642	0.973	0.742	0.974	0.987	0.989	0.944
	$\mathbb{P}[D_T < 0.05]$	0.939	0.992	0.997	0.406	0.795	0.203	0.695	0.991	0.998	0.999	0.993
	Accuracy	0.582	0.584	0.581	0.647	0.647	0.647	0.739	0.787	0.787	0.780	0.787
Text/Doc VQA	$\rho(V_\ell, V_{\ell-1})$	0.034	0.022	0.022	0.052	0.042	0.074	0.042	0.022	0.016	0.017	0.031
	$\rho(T_\ell, T_{\ell-1})$	0.032	0.018	0.020	0.047	0.032	0.058	0.045	0.023	0.013	0.014	0.022
	$\mathbb{P}[D_V < 0.05]$	0.859	0.976	0.995	0.497	0.731	0.119	0.669	0.975	0.982	0.985	0.920
	$\mathbb{P}[D_T < 0.05]$	0.871	0.985	0.978	0.405	0.796	0.204	0.593	0.989	0.997	0.996	0.981
	Accuracy	0.592	0.594	0.595	0.684	0.701	0.701	0.691	0.710	0.708	0.708	0.708
Multimodal Reasoning (Guessing)	$\rho(V_\ell, V_{\ell-1})$	0.030	0.019	0.021	0.048	0.033	0.058	0.039	0.021	0.015	0.016	0.030
	$\rho(T_\ell, T_{\ell-1})$	0.036	0.024	0.027	0.052	0.042	0.072	0.053	0.025	0.016	0.017	0.026
	$\mathbb{P}[D_V < 0.05]$	0.912	0.989	0.998	0.479	0.720	0.128	0.696	0.973	0.994	0.997	0.927
	$\mathbb{P}[D_T < 0.05]$	0.829	0.959	0.916	0.401	0.778	0.210	0.412	0.985	0.996	0.996	0.956
	Accuracy	0.248	0.248	0.248	0.234	0.237	0.238	0.245	0.263	0.262	0.264	0.263
Multimodal Reasoning (Not Guessing)	$\rho(V_\ell, V_{\ell-1})$	0.036	0.024	0.022	0.051	0.044	0.075	0.041	0.023	0.018	0.018	0.029
	$\rho(T_\ell, T_{\ell-1})$	0.032	0.020	0.022	0.046	0.031	0.056	0.046	0.022	0.014	0.014	0.022
	$\mathbb{P}[D_V < 0.05]$	0.822	0.964	0.996	0.530	0.689	0.090	0.721	0.978	0.990	0.991	0.941
	$\mathbb{P}[D_T < 0.05]$	0.905	0.977	0.959	0.327	0.798	0.203	0.599	0.991	0.995	0.997	0.981
	Accuracy	0.322	0.325	0.326	0.343	0.341	0.342	0.313	0.335	0.335	0.335	0.333

Table 2: Summary of results for early stopping on vision and textual tokens. In this table, we only focus on the layers starting on the 20th layer of each model. Before this point, early skipping causes significant performance degradation across models due to being to visual information still being processed, which is supported in Figure 3. We include layer 20 to see how are framework is applicable when VAR is moderate). In this table, accuracy in bold indicates closeness to the baseline performance.

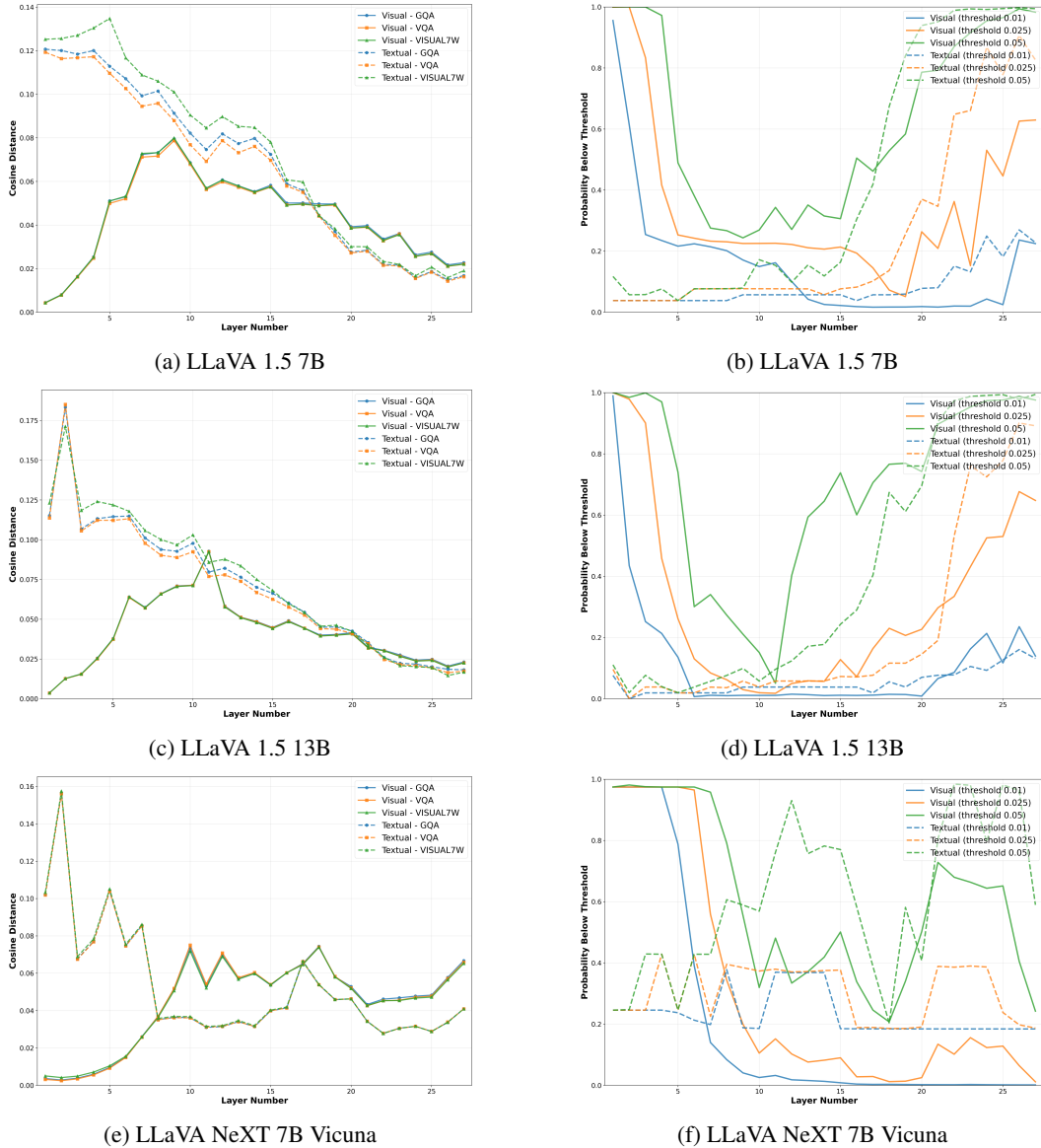


Figure 4: Empirical geometric and proximal redundancy experiments across layers for the LLaVA 1.5 7B/13B and LLaVA NeXT 7B. Across all the General VQA task (see Table 3) and models, the early layer vision tokens have low adjacent token cosine distances, and the textual and visual tokens have low adjacent token cosine distances in later layers.

Tables 1 and 2 show that performance degradation occurs once the conditions are broken. We see figures of this degradation during late entry skipping in Section D of the appendix. Since roughly the same layers can be skipped across different models, this suggests that early and late visual information is processed in a general and consistent way across VLMs, indicating a shared mechanism of reasoning about image understanding.

6 CONCLUSION & DISCUSSION

In this work, we propose a theoretical framework to study redundancies in VLMs. We then demonstrate that empirically verifiable notions of redundancy, namely average cosine distance and small cosine distance, with high probability imply more informative notions of redundancy. By combining these results with cross-attention analysis, we identify redundant layers in the model with respect

to multimodal processing and experimentally show that these redundant layers appear in the early vision tokens, late vision tokens, and late textual tokens. We then validate these findings by skipping these layers and finding minimal performance degradation across different tasks. Conversely, we also show that skipping non-redundant layers severely degrades model performance.

Future work includes further validation our results by expanding the scope of our experiments on more datasets and models. Additionally, it would be interesting to study the factors underlying dramatic instances of VLM hallucination, based on recent observations and datasets in literature (Vo et al., 2025), through the lens of our framework. A longer term pursuit would perhaps be understanding why these redundancies exist and whether they arise as a drawback of vision-language pretraining strategies, or as an intentional mechanism for multimodal processing.

REFERENCES

Aishwarya Agrawal, Jiasen Lu, Stanislaw Antol, Margaret Mitchell, C. Lawrence Zitnick, Dhruv Batra, and Devi Parikh. VQA: Visual question answering. In *Proc. IEEE Int. Conf. Comput. Vis. (ICCV)*, pp. 4548–4556, 2015. URL <https://arxiv.org/abs/1505.00468>.

Jean-Baptiste Alayrac, Jeff Donahue, Pauline Luc, Antoine Miech, Iain Barr, Yana Hasson, Karel Lenc, Arthur Mensch, Katherine Millican, Malcolm Reynolds, Roman Ring, Eliza Rutherford, Serkan Cabi, Tengda Han, Zhitao Gong, Sina Samangooei, Marianne Monteiro, Jacob Menick, Sebastian Borgeaud, Andrew Brock, Aida Nematzadeh, Sahand Sharifzadeh, Mikolaj Binkowski, Ricardo Barreira, Oriol Vinyals, Andrew Zisserman, and Karen Simonyan. Flamingo: a visual language model for few-shot learning. In *Proc. Neural Inf. Process. Sys. (NeurIPS)*, 2022. URL <https://openreview.net/forum?id=EbMuimAbPbs>.

Mikel Artetxe, Shruti Bhosale, Naman Goyal, Todor Mihaylov, Myle Ott, Sam Shleifer, Xi Victoria Lin, Jingfei Du, Srinivasan Iyer, Ramakanth Pasunuru, Giridharan Anantharaman, Xian Li, Shuhui Chen, Halil Akin, Mandeep Baines, Louis Martin, Xing Zhou, Punit Singh Koura, Brian O’Horo, Jeffrey Wang, Luke Zettlemoyer, Mona Diab, Zornitsa Kozareva, and Veselin Stoyanov. Efficient large scale language modeling with mixtures of experts. In *Proc. Conf. Empirical Methods Natural Language Process. (EMNLP)*, pp. 11699–11732, 2022. URL <https://aclanthology.org/2022.emnlp-main.804/>.

Jinze Bai, Shuai Bai, Shusheng Yang, Shijie Wang, Sinan Tan, Peng Wang, Junyang Lin, Chang Zhou, and Jingren Zhou. Qwen-VL: A versatile vision-language model for understanding, localization, text reading, and beyond. arXiv:2308.12966 [cs.CV], 2023.

Hangbo Bao, Wenhui Wang, Li Dong, Qiang Liu, Owais Khan Mohammed, Kriti Aggarwal, Subhajit Som, and Furu Wei. VLMo: Unified vision-language pre-training with mixture-of-modality-experts. arXiv:2111.02358 [cs.CV], 2022. URL <https://arxiv.org/abs/2111.02358>.

Samyadeep Basu, Martin Grayson, Cecily Morrison, Besmira Nushi, Soheil Feizi, and Daniela Massiceti. Understanding information storage and transfer in multi-modal large language models. In *Proc. Neural Inf. Process. Sys. (NeurIPS)*, 2024. URL <https://openreview.net/forum?id=s63dtq0mwA>.

Nils Bertschinger, Johannes Rauh, Eckehard Olbrich, Jürgen Jost, and Nihat Ay. Quantifying unique information. *Entropy*, 16(4):2161–2183, 2014.

Dan Biderman, Jacob Portes, Jose Javier Gonzalez Ortiz, Mansheej Paul, Philip Greengard, Connor Jennings, Daniel King, Sam Havens, Vitaliy Chiley, Jonathan Frankle, Cody Blakeney, and John Patrick Cunningham. LoRA learns less and forgets less. *Trans. Machine Learning Res.*, 2024. ISSN 2835-8856. URL <https://openreview.net/forum?id=aloEru2qCG>.

Gábor Braun and Sebastian Pokutta. An information diffusion Fano inequality. arXiv:1504.05492 [cs.IT], 2015. URL <https://arxiv.org/abs/1504.05492>.

Liang Chen, Haozhe Zhao, Tianyu Liu, Shuai Bai, Junyang Lin, Chang Zhou, and Baobao Chang. An image is worth 1/2 tokens after layer 2: Plug-and-play inference acceleration for large vision-language models. In *Proc. Eur. Conf. Comput. Vis. (ECCV)*, pp. 19–35, 2024a.

Lin Chen, Jinsong Li, Xiaoyi Dong, Pan Zhang, Yuhang Zang, Zehui Chen, Haodong Duan, Jiaqi Wang, Yu Qiao, Dahua Lin, and Feng Zhao. Are we on the right way for evaluating large vision-language models? In *Proc. Neural Inf. Process. Sys. (NeurIPS)*, 2024b.

Moulik Choraria, Xinbo Wu, Akhil Bhimaraju, Nitesh Sekhar, Yue Wu, Xu Zhang, Prateek Singhal, and Lav R. Varshney. DeepInsert: Early layer bypass for efficient and performant multimodal understanding. arXiv:2504.19327 [cs.CV], 2025. URL <https://arxiv.org/abs/2504.19327>.

Matt Deitke, Christopher Clark, Sangho Lee, Rohun Tripathi, Yue Yang, Jae Sung Park, Mohammadreza Salehi, Niklas Muennighoff, Kyle Lo, Luca Soldaini, Jiasen Lu, Taira Anderson, Erin Bransom, Kiana Ehsani, Huong Ngo, YenSung Chen, Ajay Patel, Mark Yatskar, Chris Callison-Burch, Andrew Head, Rose Hendrix, Favyen Bastani, Eli VanderBilt, Nathan Lambert, Yvonne Chou, Arnavi Chheda, Jenna Sparks, Sam Skjonsberg, Michael Schmitz, Aaron Sarnat, Byron Bischoff, Pete Walsh, Chris Newell, Piper Wolters, Tanmay Gupta, Kuo-Hao Zeng, Jon Borchartd, Dirk Groeneveld, Crystal Nam, Sophie Lebrecht, Caitlin Wittlif, Carissa Schoenick, Oscar Michel, Ranjay Krishna, Luca Weihs, Noah A. Smith, Hannaneh Hajishirzi, Ross Girshick, Ali Farhadi, and Aniruddha Kembhavi. Molmo and PixMo: Open weights and open data for state-of-the-art vision-language models. In *Proc. IEEE/CVF Conf. Comput. Vis. Pattern Recognition (CVPR)*, pp. 91–104, 2025.

Tim Dettmers, Artidoro Pagnoni, Ari Holtzman, and Luke Zettlemoyer. QLoRA: Efficient finetuning of quantized LLMs. arXiv:2305.14314 [cs.LG], 2023. URL <https://arxiv.org/abs/2305.14314>.

Pasan Dissanayake, Faisal Hamman, Barproda Halder, Ilia Sucholutsky, Qiuyi Zhang, and Sanghamitra Dutta. Quantifying knowledge distillation using partial information decomposition. arXiv:2411.07483 [stat.ML], 2025. URL <https://arxiv.org/abs/2411.07483>.

John C. Duchi and Martin J. Wainwright. Distance-based and continuum Fano inequalities with applications to statistical estimation. arXiv:1311.2669 [cs.IT], 2013. URL <https://arxiv.org/abs/1311.2669>.

Mostafa Elhoushi, Akshat Shrivastava, Diana Liskovich, Basil Hosmer, Bram Wasti, Liangzhen Lai, Anas Mahmoud, Bilge Acun, Saurabh Agarwal, Ahmed Roman, Ahmed Aly, Beidi Chen, and Carole-Jean Wu. LayerSkip: Enabling early exit inference and self-speculative decoding. In *Proc. Association Computational Linguistics (ACL)*, pp. 12622–12642, 2024. URL <https://dx.doi.org/10.18653/v1/2024.acl-long.681>.

Zhuomin He, Yizhen Yao, Pengfei Zuo, Bin Gao, Qinya Li, Zhenzhe Zheng, and Fan Wu. AdaSkip: Adaptive sublayer skipping for accelerating long-context LLM inference. *Proc. AAAI Conf. Artificial Intel.*, 39(22):24050–24058, 2025.

Edward J. Hu, Yelong Shen, Phillip Wallis, Zeyuan Allen-Zhu, Yuanzhi Li, Shean Wang, Lu Wang, and Weizhu Chen. LoRA: Low-rank adaptation of large language models. In *Proc. Int. Conf. Learning Representations (ICLR)*, 2022. URL <https://openreview.net/forum?id=nZeVKeeFYf9>.

Drew A. Hudson and Christopher D. Manning. GQA: a new dataset for real-world visual reasoning and compositional question answering. In *Proc. IEEE/CVF Conf. Comput. Vis. Pattern Recog. (CVPR)*, 2019. doi: 10.1109/cvpr.2019.00686.

Zhangqi Jiang, Junkai Chen, Beier Zhu, Tingjin Luo, Yankun Shen, and Xu Yang. Devils in middle layers of large vision-language models: Interpreting, detecting and mitigating object hallucinations via attention lens. In *Proc. Comput. Vis. Pattern Recog. (CVPR)*, pp. 25004–25014, 2025.

Yizhang Jin, Jian Li, Yexin Liu, Tianjun Gu, Kai Wu, Zhengkai Jiang, Muyang He, Bo Zhao, Xin Tan, Zhenye Gan, Yabiao Wang, Chengjie Wang, and Lizhuang Ma. Efficient multimodal large language models: A survey. arXiv:2405.10739 [cs.CV], 2024. URL <https://arxiv.org/abs/2405.10739>.

Aniruddha Kembhavi, Mike Salvato, Eric Kolve, Minjoon Seo, Hannaneh Hajishirzi, and Ali Farhadi. A diagram is worth a dozen images. In *Proc. Eur. Conf. Comput. Vis. (ECCV)*, 2016.

Junnan Li, Dongxu Li, Caiming Xiong, and Steven Hoi. BLIP: Bootstrapping language-image pre-training for unified vision-language understanding and generation. In *Proc. Int. Conf. Machine Learning (ICML)*, volume 162, pp. 12888–12900, 2022.

Junnan Li, Dongxu Li, Silvio Savarese, and Steven Hoi. BLIP-2: Bootstrapping language-image pre-training with frozen image encoders and large language models. In *Proc. Int. Conf. Machine Learning (ICML)*, volume 202, pp. 19730–19742, 2023.

Bin Lin, Zhenyu Tang, Yang Ye, Jinfa Huang, Junwu Zhang, Yatian Pang, Peng Jin, Munan Ning, Jiebo Luo, and Li Yuan. MoE-LLaVA: Mixture of experts for large vision-language models. arXiv:2401.15947 [cs.CV], 2024. URL <https://arxiv.org/abs/2401.15947>.

Zhihang Lin, Mingbao Lin, Luxi Lin, and Rongrong Ji. Boosting multimodal large language models with visual tokens withdrawal for rapid inference. In *Proc. AAAI Conf. Artificial Intel.*, pp. 5334–5342, 2025.

Haotian Liu, Chunyuan Li, Qingyang Wu, and Yong Jae Lee. Visual instruction tuning. In *Proc. Neural Inf. Process. Sys. (NeurIPS)*, volume 36, pp. 34892–34916, 2023.

Haotian Liu, Chunyuan Li, Yuheng Li, Bo Li, Yuanhan Zhang, Sheng Shen, and Yong Jae Lee. LLaVA-NeXT: Improved reasoning, OCR, and world knowledge, 2024a. URL <https://llava-vl.github.io/blog/2024-01-30-llava-next/>.

Yuliang Liu, Zhang Li, Mingxin Huang, Biao Yang, Wenwen Yu, Chunyuan Li, Xu-Cheng Yin, Cheng-Lin Liu, Lianwen Jin, and Xiang Bai. OCRBench: On the hidden mystery of OCR in large multimodal models. *Sci. China Inf. Sci.*, 2024b.

Zhijian Liu, Ligeng Zhu, Baifeng Shi, Zhuoyang Zhang, Yuming Lou, Shang Yang, Haocheng Xi, Shiyi Cao, Yuxian Gu, Dacheng Li, Xiuyu Li, Yunhao Fang, Yukang Chen, Cheng-Yu Hsieh, De-An Huang, An-Chieh Cheng, Vishwesh Nath, Andriy Myronenko, Jinyi Hu, Sifei Liu, Ranjay Krishna, Daguang Xu, Xiaolong Wang, Pavlo Molchanov, Jan Kautz, Hongxu Yin, Song Han, and Yao Lu. NVILA: Efficient frontier visual language models. In *Proc. IEEE/CVF Conf. Comput. Vis. Pattern Recog. (CVPR)*, pp. 3861–3872, 2025.

Haoyu Lu, Wen Liu, Bo Zhang, Bingxuan Wang, Kai Dong, Bo Liu, Jingxiang Sun, Tongzheng Ren, Zhuoshu Li, Hao Yang, Yaofeng Sun, Chengqi Deng, Hanwei Xu, Zhenda Xie, and Chong Ruan. DeepSeek-VL: Towards real-world vision-language understanding. arXiv:2403.05525 [cs.AI], 2024.

Xuan Luo, Weizhi Wang, and Xifeng Yan. Adaptive layer-skipping in pre-trained LLMs. In *Proc. Conf. Language Modeling (COLM)*, 2025a. URL <https://arxiv.org/abs/2503.23798>.

Yixin Luo, Gen Luo, Jiayi Ji, Yiyi Zhou, Xiaoshuai Sun, Zhiqiang Shen, and Rongrong Ji. γ -MoD: Exploring mixture-of-depth adaptation for multimodal large language models. In *Proc. Int. Conf. Learning Representations (ICLR)*, 2025b. URL <https://openreview.net/forum?id=q44uq3tc2D>.

Kevin Meng, David Bau, Alex J Andonian, and Yonatan Belinkov. Locating and editing factual associations in GPT. In *Proc. Neural Inf. Process. Sys. (NeurIPS)*, 2022. URL <https://openreview.net/forum?id=-h6WAS6eE4>.

Kevin Meng, Arnab Sen Sharma, Alex J Andonian, Yonatan Belinkov, and David Bau. Mass-editing memory in a transformer. In *Proc. Int. Conf. Learning Representations (ICLR)*, 2023. URL <https://openreview.net/forum?id=MkbcAHIYgyS>.

Meta AI. The Llama 4 herd: The beginning of a new era of natively multimodal AI innovation, 2024. URL <https://ai.meta.com/blog/llama-4-multimodal-intelligence/>.

Clement Neo, Luke Ong, Philip Torr, Mor Geva, David Krueger, and Fazl Barez. Towards interpreting visual information processing in vision-language models. In *Proc. Int. Conf. Learning Representations (ICLR)*, 2025. URL <https://openreview.net/forum?id=chanJGoa7f>.

Nostalgebraist. Interpreting GPT: The logit lens. <https://www.alignmentforum.org/posts/AcKRB8wDpdaN6v6ru/interpreting-gpt-the-logit-lens>, 2020. Accessed: 23 Sep 2024.

OpenAI. GPT-5 system card. <https://cdn.openai.com/gpt-5-system-card.pdf>, 2025. Accessed: Sep 24, 2025.

Qwen, An Yang, Baosong Yang, Beichen Zhang, Binyuan Hui, Bo Zheng, Bowen Yu, Chengyuan Li, Dayiheng Liu, Fei Huang, Haoran Wei, Huan Lin, Jian Yang, Jianhong Tu, Jianwei Zhang, Jianxin Yang, Jiaxi Yang, Jingren Zhou, Junyang Lin, Kai Dang, Keming Lu, Keqin Bao, Kexin Yang, Le Yu, Mei Li, Mingfeng Xue, Pei Zhang, Qin Zhu, Rui Men, Runji Lin, Tianhao Li, Tianyi Tang, Tingyu Xia, Xingzhang Ren, Xuancheng Ren, Yang Fan, Yang Su, Yichang Zhang, Yu Wan, Yuqiong Liu, Zeyu Cui, Zhenru Zhang, and Zihan Qiu. Qwen2.5 technical report. arXiv:2412.15115 [cs.CL], 2025. URL <https://arxiv.org/abs/2412.15115>.

Alec Radford, Jong Wook Kim, Chris Hallacy, Aditya Ramesh, Gabriel Goh, Sandhini Agarwal, Girish Sastry, Amanda Askell, Pamela Mishkin, Jack Clark, Gretchen Krueger, and Ilya Sutskever. Learning transferable visual models from natural language supervision. In *Proc. Int. Conf. Machine Learning (ICML)*, volume 139, pp. 8748–8763, 2021.

Yuzhang Shang, Mu Cai, Bingxin Xu, Yong Jae Lee, and Yan Yan. LLaVA-PruMerge: Adaptive token reduction for efficient large multimodal models. In *Proc. IEEE Int. Conf. Comput. Vis. (ICCV)*, 2025. URL <https://arxiv.org/abs/2403.15388>.

Amanpreet Singh, Vivek Natarjan, Meet Shah, Yu Jiang, Xinlei Chen, Devi Parikh, and Marcus Rohrbach. Towards VQA models that can read. In *Proc. IEEE Conf. Comput. Vis. Pattern Recog. (CVPR)*, pp. 8317–8326, 2019.

Pavan Kumar Anasosalu Vasu, Fartash Faghri, Chun-Liang Li, Cem Koc, Nate True, Albert Antony, Gokul Santhanam, James Gabriel, Peter Grasch, Oncel Tuzel, and Hadi Pouransari. FastVLM: Efficient vision encoding for vision language models. In *Proc. IEEE/CVF Conf. Comput. Vis. Pattern Recognition (CVPR)*, 2025.

An Vo, Khai-Nguyen Nguyen, Mohammad Reza Taesiri, Vy Tuong Dang, Anh Totti Nguyen, and Daeyoung Kim. Vision language models are biased: Counting legs of an animal is surprisingly hard. In *Proc. AI for Math Workshop @ ICML*, 2025. URL <https://openreview.net/forum?id=O2xoCaU6nS>.

Ke Wang, Junting Pan, Weikang Shi, Zimu Lu, Houxing Ren, Aojun Zhou, Mingjie Zhan, and Hongsheng Li. Measuring multimodal mathematical reasoning with MATH-vision dataset. In *Proc. Neural Inf. Process. Sys. (NeurIPS) Datasets and Benchmarks Track*, 2024.

xAI. RealWorldQA. <https://huggingface.co/datasets/xai-org/RealworldQA>, 2024. Hugging Face Dataset.

Yilun Xu, Shengjia Zhao, Jiaming Song, Russell Stewart, and Stefano Ermon. A theory of usable information under computational constraints. In *Proc. Int. Conf. Learning Representations (ICLR)*, 2020. URL <https://openreview.net/forum?id=r1eBeyHFDH>.

Xiang Yue, Yuansheng Ni, Kai Zhang, Tianyu Zheng, Ruoqi Liu, Ge Zhang, Samuel Stevens, Dongfu Jiang, Weiming Ren, Yuxuan Sun, Cong Wei, Botao Yu, Ruibin Yuan, Renliang Sun, Ming Yin, Boyuan Zheng, Zhenzhu Yang, Yibo Liu, Wenhao Huang, Huan Sun, Yu Su, and Wenhui Chen. MMMU: A massive multi-discipline multimodal understanding and reasoning benchmark for expert AGI. In *Proc. IEEE Conf. Comput. Vis. Pattern Recog. (CVPR)*, 2024.

Xiaohua Zhai, Basil Mustafa, Alexander Kolesnikov, and Lucas Beyer. Sigmoid loss for language image pre-training. In *Proc. IEEE/CVF Int. Conf. Comput. Vis. (ICCV)*, pp. 11975–11986, 2023.

Rongyu Zhang, Menghang Dong, Yuan Zhang, Liang Heng, Xiaowei Chi, Gaole Dai, Li Du, Yuan Du, and Shanghang Zhang. MoLe-VLA: Dynamic layer-skipping vision language action model via mixture-of-layers for efficient robot manipulation. arXiv:2503.20384 [cs.RO], 2025.

Yuke Zhu, Oliver Groth, Michael Bernstein, and Li Fei-Fei. Visual7W: Grounded question answering in images. In *Proc. IEEE Conf. Comput. Vis. Pattern Recognition (CVPR)*, 2016.

APPENDIX

A PROOFS

A.1 PROOFS OF LEMMAS

Lemma 1. Let (X, d) be a metric space and $x, y, z \in X$. Then $d(x, y)^2 \leq 2d(x, z)^2 + 2d(z, y)^2$.

Proof. Follows from the triangle inequality and the AM-GM inequality. \square

Lemma 2. Suppose X, Y are random vectors with unit norm (with probability 1). Let $\rho(x, y) = 1 - \frac{\langle x, y \rangle}{\|x\| \|y\|}$ be the cosine distance between x and y . Then $\mathbb{E}[\rho(X, Y)] < \frac{\epsilon}{2}$ implies $\mathbb{E}[\|X - Y\|_2^2] < \epsilon$.

Proof. Observe that

$$\mathbb{E}[\|X - Y\|_2^2] = \mathbb{E}[\|X\|^2 + \|Y\|^2 - 2\langle X, Y \rangle] = 2\mathbb{E}[1 - \langle X, Y \rangle] \quad (4)$$

$$= 2\mathbb{E}[\rho(X, Y)] \quad (5)$$

$$< \epsilon. \quad (6)$$

\square

Lemma 3. Let $(X, \langle \cdot, \cdot \rangle)$ be a real inner product space and $a, b, c \in X$. Then $\|a + b + c\|^2 \leq 3(\|a\|^2 + \|b\|^2 + \|c\|^2)$.

Proof. Expanding $\|a + b + c\|^2$ we get $\|a\|^2 + \|b\|^2 + \|c\|^2 + 2\langle a, b \rangle + 2\langle b, c \rangle + 2\langle a, c \rangle$. Thus we want to show that $0 \leq 2\|a\|^2 + 2\|b\|^2 + 2\|c\|^2 - 2\langle a, b \rangle - 2\langle b, c \rangle - 2\langle a, c \rangle$. This is equivalent to showing $0 \leq \|a - b\|^2 + \|b - c\|^2 + \|a - c\|^2$ and since $\|\cdot\|^2$ is non-negative, we are done. \square

Lemma 4. Suppose $Y - X - Z$ is a Markov chain. Then $\mathbb{E}_{(X, Y)}[D(p_{Z|X} || p_{Z|Y})] = I(Z; X|Y)$.

Proof. Observe that

$$\mathbb{E}[D(p_{Z|X} || p_{Z|Y})] = \mathbb{E} \left[\int p_{Z|X}(z|X) \log \frac{p_{Z|X}(z|X)}{p_{Z|Y}(z|Y)} dz \right] \quad (7)$$

$$= \mathbb{E}_{(X, Y), Z \sim p(\cdot|X)} \left[\log \frac{p(Z|X)}{p(Z|Y)} \right] \quad (8)$$

$$= \mathbb{E}_{(X, Y), Z \sim p(\cdot|X, Y)} \left[\log \frac{p(Z|X, Y)}{p(Z|Y)} \right] \quad (9)$$

$$= \mathbb{E}_{X, Y, Z} \left[\log \frac{p(Z, X|Y)}{p(X|Y)p(Z|Y)} \right] \quad (10)$$

$$= I(Z; X|Y) \quad (11)$$

where equation 9 follows from the Markov property and equation 11 is the definition of conditional mutual information. \square

A.2 PROOFS OF PROPOSITIONS AND THEOREMS

Proposition 1. Let $\rho : \mathcal{X} \times \mathcal{X} \rightarrow \mathbb{R}$ be a symmetric function with $0 \leq \rho \leq 1$. Then

$$\mathbb{P}[\rho(X, Y) > t] < \frac{\epsilon - t}{1 - t} \text{ implies } \mathbb{E}[\rho(X, Y)] < \epsilon \quad (11)$$

Proof. Define the random variable $D := \rho(X, Y)$. By the tail integration formula,

$$\mathbb{E}[D] = \int_0^1 \mathbb{P}[D > s] ds \quad (12)$$

$$= \int_0^t \mathbb{P}[D > s] ds + \int_t^1 \mathbb{P}[D > s] ds \quad (13)$$

$$\leq t \cdot 1 + (1-t)\mathbb{P}[D > t] \quad (14)$$

$$< t + (1-t)\left(\frac{\epsilon - t}{1-t}\right) \quad (15)$$

$$= \epsilon. \quad (16)$$

□

Theorem 1. Let $X_\ell, X_{\ell-1}$ be unit-norm random variables and Z be another random variable (e.g. hidden representations of layers $\ell, \ell-1$ and the task ground truth respectively). Let $\rho(x, y) = 1 - \frac{\langle x, y \rangle}{\|x\| \|y\|}$. Assume $\mathbb{E}[\rho(X, Y)] < \frac{\epsilon}{2}$ and that

$$h(x, y) = E[Z|X_\ell = x, X_{\ell-1} = y].$$

is α -Lipschitz in the first argument and β -Lipschitz in the second. Then $E[\|E[Z|X_\ell] - E[Z|X_{\ell-1}]\|_2^2] < 2(\alpha^2 + \beta^2)\epsilon$.

Proof. Observe that

$$\mathbb{E}[Z|X_\ell] - E[Z|X_{\ell-1}] = \mathbb{E}[\mathbb{E}[Z|X_\ell, X_{\ell-1}]|X_\ell] - \mathbb{E}[\mathbb{E}[Z|X_\ell, X_{\ell-1}]|X_{\ell-1}] \quad (17)$$

$$= \mathbb{E}[h|X_\ell] - \mathbb{E}[h|X_{\ell-1}] \quad (18)$$

By Lemma 2 we have that $\mathbb{E}[\|X_\ell - X_{\ell-1}\|_2^2] < \epsilon$ since $\|X_\ell\|$ and $\|X_{\ell-1}\|$ are unit-norm. By Lemma 1 we have

$$(\mathbb{E}[h|X_\ell] - \mathbb{E}[h|X_{\ell-1}])^2 \leq 2(\mathbb{E}[h|X_\ell] - h)^2 + 2(\mathbb{E}[h|X_{\ell-1}] - h)^2$$

Furthermore, since expectation is order-preserving, we have

$$\mathbb{E}[(\mathbb{E}[h|X_\ell] - \mathbb{E}[h|X_{\ell-1}])^2] \leq 2\mathbb{E}[(\mathbb{E}[h|X_\ell] - h)^2] + 2\mathbb{E}[(\mathbb{E}[h|X_{\ell-1}] - h)^2] \quad (19)$$

$$= 2\mathbb{E}[\text{Var}(h|X_\ell)] + 2\mathbb{E}[\text{Var}(h|X_{\ell-1})] \quad (20)$$

By definition,

$$\mathbb{E}[\text{Var}(h(X_\ell, X_{\ell-1})|X_\ell = x)] = \mathbb{E}[\mathbb{E}[(h(X_\ell, X_{\ell-1}) - \mathbb{E}[h(X_\ell, X_{\ell-1})|X_\ell = x])^2|X_\ell = x]] \quad (21)$$

$$\leq \mathbb{E}[\mathbb{E}[(h(X_\ell, X_{\ell-1}) - h(X_\ell, X_{\ell-1} = \mathbb{E}[X_{\ell-1}|X_\ell = x]))^2|X_\ell = x]] \quad (22)$$

$$\leq \beta^2 \mathbb{E}[\mathbb{E}[\|X_{\ell-1} - \mathbb{E}[X_{\ell-1}|X_\ell = x]\|_2^2|X_\ell = x]] \quad (23)$$

$$= \beta^2 \mathbb{E}[\|X_{\ell-1} - \mathbb{E}[X_{\ell-1}|X_\ell = x]\|_2^2] \quad (24)$$

$$\leq \beta^2 \mathbb{E}[\|X_{\ell-1} - X_\ell\|_2^2] \quad (25)$$

$$< \beta^2 \epsilon \quad (26)$$

where equation 22 holds by the optimality of the minimum mean squared error (MMSE) estimator, equation 23 holds by the Lipschitz assumption, equation 24 holds by the tower property (Law of Total Expectation), and equation 25 holds by the optimality of the MMSE estimator once again. By symmetry, the same holds $X_{\ell-1}$ (i.e. $\mathbb{E}[\text{Var}(h|X_{\ell-1} = y)] < \alpha^2 \epsilon$) so $\mathbb{E}[(\mathbb{E}[Z|X_\ell] - \mathbb{E}[Z|X_{\ell-1}])^2] \leq 2(\alpha^2 + \beta^2)\epsilon$ □

Theorem 2. Let $X_\ell, X_{\ell-1}$ be unit-norm random variables and Z be another random variable (e.g. layer activations of layers $\ell, \ell-1$ and a task variable respectively). Let $\rho(x, y) = 1 - \frac{\langle x, y \rangle}{\|x\| \|y\|}$. Assume $\mathbb{E}[\rho(X, Y)] < \frac{\epsilon}{2}$ and that

$$h(x, y) = E[Z|X_\ell = x, X_{\ell-1} = y]$$

is α -Lipschitz in the first argument and β -Lipschitz in the second. Let \hat{f}_ℓ is a finite-sample estimate of $f_\ell^*(x) = \mathbb{E}[Z|X_\ell = x]$ and $\hat{f}_{\ell-1}(x)$ is a finite-sample estimate of $f_{\ell-1}^*(x) = \mathbb{E}[Z|X_{\ell-1} = x]$. Further let, $\eta_\ell = \mathbb{E}[\|\hat{f}_\ell(X_\ell) - f_\ell^*(X_\ell)\|^2]$ and $\eta_{\ell-1} = \mathbb{E}[\|\hat{f}_{\ell-1}(X_{\ell-1}) - f_{\ell-1}^*(X_{\ell-1})\|^2]$. We then have

$$\mathbb{E}[\|\hat{f}_\ell(X_\ell) - \hat{f}_{\ell-1}(X_{\ell-1})\|^2] < 3\eta_\ell + 3\eta_{\ell-1} + 6(\alpha^2 + \beta^2)\epsilon$$

Proof. By Lemma 2 we have that $\mathbb{E}[\|X_\ell - X_{\ell-1}\|_2^2] < \epsilon$.

Observe that

$$\hat{f}_\ell(X_\ell) - \hat{f}_{\ell-1}(X_{\ell-1}) = (-f_\ell^*(X_\ell) + \hat{f}_\ell(X_\ell)) + (f_{\ell-1}^*(X_{\ell-1}) - \hat{f}_{\ell-1}(X_{\ell-1})) + (f_\ell^*(X_\ell) - f_{\ell-1}^*(X_{\ell-1})).$$

Thus by Lemma 3 we have:

$$\|\hat{f}_\ell(X_\ell) - \hat{f}_{\ell-1}(X_{\ell-1})\|^2 \leq 3(\|f_\ell^*(X_\ell) - \hat{f}_\ell(X_\ell)\|^2 + \|f_{\ell-1}^*(X_{\ell-1}) - \hat{f}_{\ell-1}(X_{\ell-1})\|^2 + \|f_\ell^*(X_\ell) - f_{\ell-1}^*(X_{\ell-1})\|^2)$$

Finally, by taking expectations we get

$$\mathbb{E}[\|\hat{f}_\ell(X_\ell) - \hat{f}_{\ell-1}(X_{\ell-1})\|^2] \leq 3(\eta_\ell + \eta_{\ell-1} + 2(L_1^2 + L_2^2)\epsilon) = 3\eta_\ell + 3\eta_{\ell-1} + 6(\alpha^2 + \beta^2)\epsilon.$$

□

Theorem 3 (Fano's Inequality; (Duchi & Wainwright, 2013)). *Let $X_\ell, X_{\ell-1}$ be random variables with shared finite support \mathcal{X} . Let $\rho : \mathcal{X} \times \mathcal{X} \rightarrow \mathbb{R}$ be a symmetric function (e.g. a metric). Let H_2 be the binary entropy function, $\overline{B}(t, x) := \{x' \in \mathcal{X} | \rho(x, x') \leq t\}$, $N_t^{\max} := \max_{x \in \mathcal{X}} \{|\overline{B}(t, x)|\}$ and $N_t^{\min} := \min_{x \in \mathcal{X}} \{|\overline{B}(t, x)|\}$. Finally, let $P_t = \mathbb{P}[\rho(X_{\ell-1}, X_\ell) > t]$. We then have that*

$$H(X_\ell | X_{\ell-1}) \leq H_2(P_t) + P_t \log \frac{|\mathcal{X}| - N_t^{\min}}{N_t^{\max}} + \log N_t^{\max}$$

Proof. Observe that $X_\ell - X_{\ell-1} - X_{\ell-1}$ is trivially a Markov chain. The result follows from applying results from Duchi & Wainwright (2013). □

Theorem 4 (Braun & Pokutta, 2015)). *Let $X_\ell, X_{\ell-1}$ be random variables with shared finite support \mathcal{X} . Let $\rho : \mathcal{X} \times \mathcal{X} \rightarrow \mathbb{R}$ be a symmetric function (e.g. a metric). Let $\overline{B}(t, x) := \{x' \in \mathcal{X} | \rho(x, x') \leq t\}$, $P_t = \mathbb{P}[\rho(X_{\ell-1}, X_\ell) > t]$. Let*

$$p_{\min} := \inf_{x \in \mathcal{X}} \mathbb{P}[(X_{\ell-1}, x) \in \overline{B}(t, x)] \text{ and } p_{\max} := \sup_{x \in \mathcal{X}} \mathbb{P}[(X_{\ell-1}, x) \in \overline{B}(t, x)]$$

with $0 \leq p_{\min} < 1$ and $0 < p_{\max} \leq 1$ and $p_{\min} + p_{\max} < 1$. Then,

$$I(X_{\ell-1}; X_\ell) \geq (1 - P_t) \log \frac{1}{p_{\max}} - P_t \log(1 - p_{\min}) - H_2(P_t)$$

Proof. Follows directly from Proposition 2.2 in Braun & Pokutta (2015) with $R = \{(x, x') \in \mathcal{X} \times \mathcal{X} : \rho(x, x') \leq t\}$. □

Theorem 5. *Suppose there are random variables $Z, X_\ell, X_{\ell-1}$ with $Z \in \mathbb{R}^d$ and $X_\ell, X_{\ell-1}$ discrete random variables. Further suppose $\|Z\|_2 \leq B$ almost surely and that $X_{\ell-1} \rightarrow X_\ell \rightarrow Z$ is a Markov Chain. Then $\mathbb{E}[\|\mathbb{E}[Z|X_\ell] - \mathbb{E}[Z|X_{\ell-1}]\|_2^2] \leq 2B^2 H(X_\ell | X_{\ell-1})$.*

Proof. Fix an a, b and consider the conditional probability distributions $p_{Z|X_\ell=a}$ and $p_{Z|X_{\ell-1}=b}$. We then have that

$$\mathbb{E}[Z|X_\ell = a] - \mathbb{E}[Z|X_{\ell-1} = b] = \int_{\mathbb{R}^d} z(p_{Z|X_\ell=a}(z) - p_{Z|X_{\ell-1}=b}(z)) dz.$$

Thus,

$$\|\mathbb{E}[Z|X_\ell = a] - \mathbb{E}[Z|X_{\ell-1} = b]\|_2 = \left\| \int_{\mathbb{R}^d} z(p_{Z|X_\ell=a}(z) - p_{Z|X_{\ell-1}=b}(z)) dz \right\|_2 \quad (27)$$

$$\leq \int_{\mathbb{R}^d} \|z\|_2 |p_{Z|X_\ell=a}(z) - p_{Z|X_{\ell-1}=b}(z)| dz \quad (28)$$

$$\leq B \int_{\mathbb{R}^d} |p_{Z|X_\ell=a}(z) - p_{Z|X_{\ell-1}=b}(z)| dz \quad (29)$$

$$= 2B\delta_{TV}(p_{Z|X_\ell=a}, p_{Z|X_{\ell-1}=b}) \quad (30)$$

where equation 28 holds by the triangle inequality. Thus we have,

$$\mathbb{E}[\|\mathbb{E}[Z|X_\ell] - \mathbb{E}[Z|X_{\ell-1}]\|_2^2] \leq 4B^2\mathbb{E}[\delta_{TV}(p_{Z|X_\ell=a}, p_{Z|X_{\ell-1}=b})^2] \quad (31)$$

$$\leq 2B^2\mathbb{E}[D(p_{Z|X_\ell}||p_{Z|X_{\ell-1}})]. \quad (32)$$

where equation 32 holds by Pinsker's inequality.

Now, by Lemma 4 we have $2B^2\mathbb{E}[D(p_{Z|X_\ell}||p_{Z|X_{\ell-1}})] = 2B^2I(Z; X_\ell|X_{\ell-1})$. Finally, we know that $I(Z; X_\ell|X_{\ell-1}) = H(X_\ell|X_{\ell-1}) - H(X_\ell|Z, X_{\ell-1}) \leq H(X_\ell|X_{\ell-1})$ because $X_\ell, X_{\ell-1}$ are discrete random variables. Thus,

$$\mathbb{E}[\|\mathbb{E}[Z|X_\ell] - \mathbb{E}[Z|X_{\ell-1}]\|_2^2] \leq 2B^2H(X_\ell|X_{\ell-1}).$$

□

B DATASETS

In this work, we experiment on General Visual Question Answering (VQA), Text/Doc VQA, Multi-modal Reasoning, and Math Reasoning. See the table below for a dataset breakdown.

Task	Datasets
General VQA	GQA, VQA, Visual7W
Text/Doc VQA	AI2D, OCRBench, TextVQA
Multimodal Reasoning	MMMU, RealWorldQA, MMStar, MathVision

Table 3: Dataset Organization by task

B.1 EVALUATION METHOD OF EACH DATASET

We split our datasets into two groups depending on whether they contain MCQ questions that can be answered in one token or not. The MCQ datasets include Visual7W, AI2D, MMMU, MMStar, and a subset of MathVision. We used an LLM-as-a-judge approach to evaluate the other datasets. These include: VQA, GQA, TextVQA, OCRBench, RealWorldQA, and a subset of MathVision.

For the MCQ datasets, we ran a forward pass to generate exactly the predicted letter (A, B, C, D). We then directly compared the predicted letter to the correct letter. Some of the datasets included Yes/No questions, and these were evaluated the same way.

For the LLM-as-a-judge datasets, we generated 256 tokens. We then used GPT-5 (OpenAI, 2025) to evaluate if the predicted answer was correct given the question and correct answer. This approach was beneficial to avoid association reasoning problems that smaller models (13B or less parameters) may have answering complex questions.

C FURTHER RESULTS FROM SECTION 4

We include experiments on Text/Doc VQA and Multimodal Reasoning task datasets on all models and more experiments on the Qwen 2.5 VL and Deepseek VL 7B to validate our results are consistent across task types.

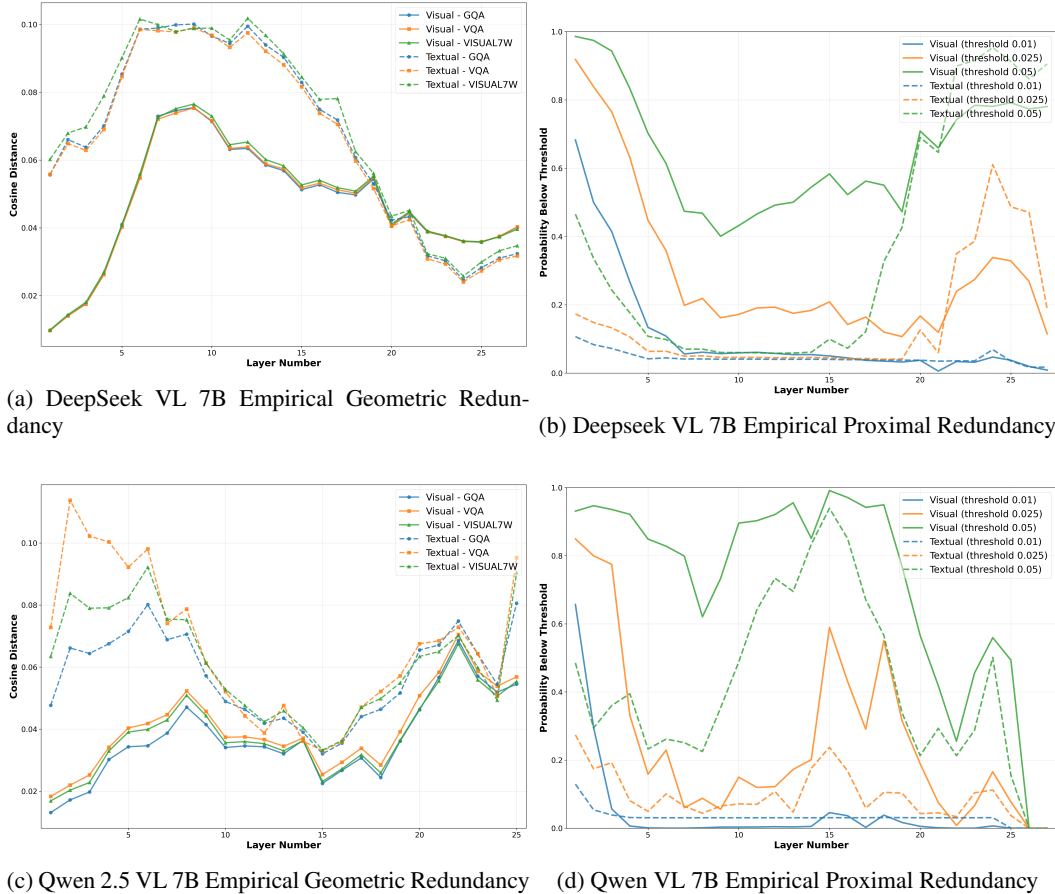


Figure 5: Empirical Geometric and Proximal Redundancy Experiments across layers for the Qwen 2.5 VL and Deepseek VL 7B VLMs. Across all datasets in the General VQA task (see Table 3) and models, the early layer vision tokens have low adjacent token cosine distances, and the textual and visual tokens have low adjacent token cosine distances in later layers.

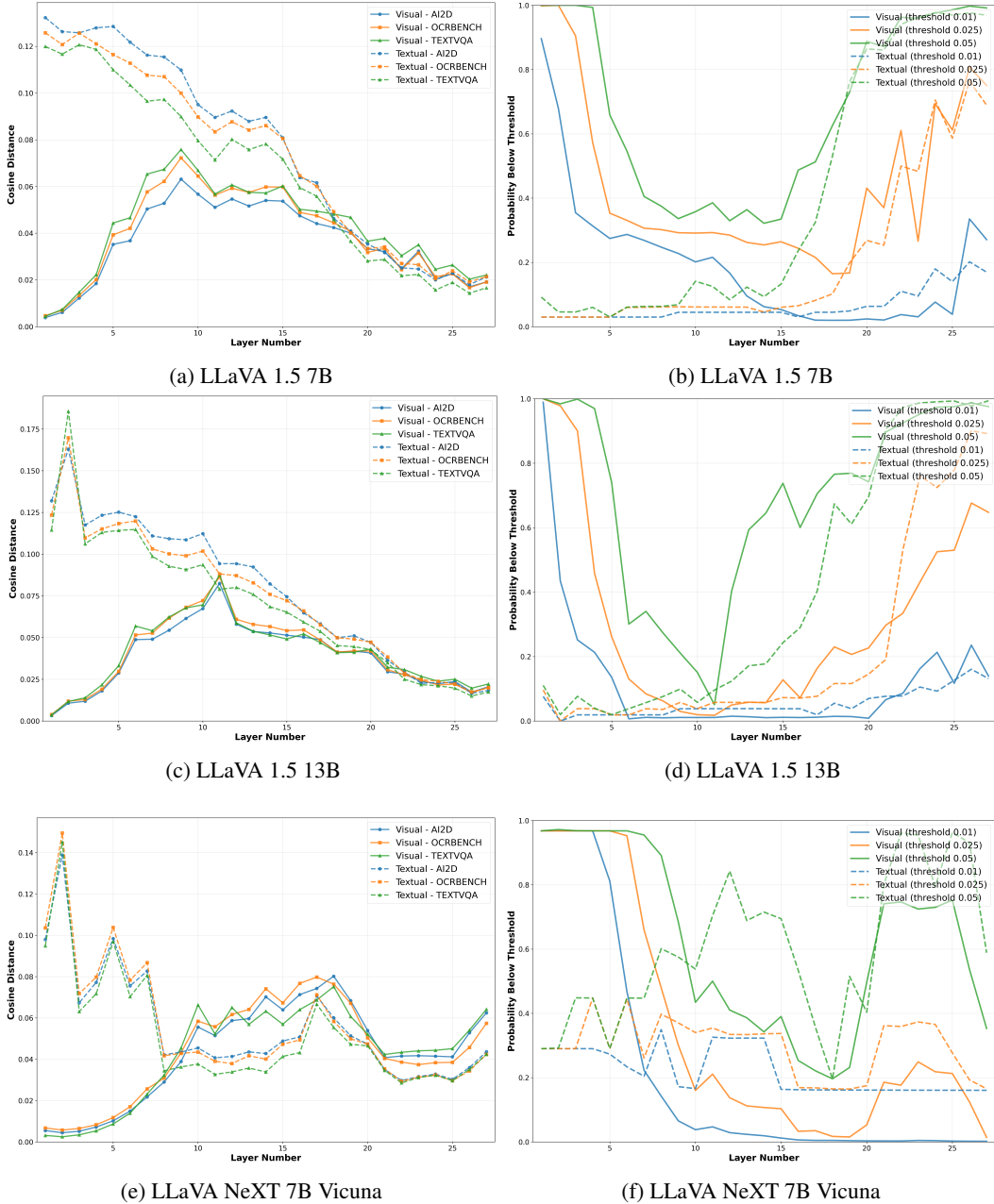


Figure 6: Empirical Geometric and Proximal Redundancy Experiments across layers for the LLaVA models. Across all datasets in the Text/Doc VQA task (see Table 3) and models, the early and late layer vision tokens have low adjacent token cosine distances.

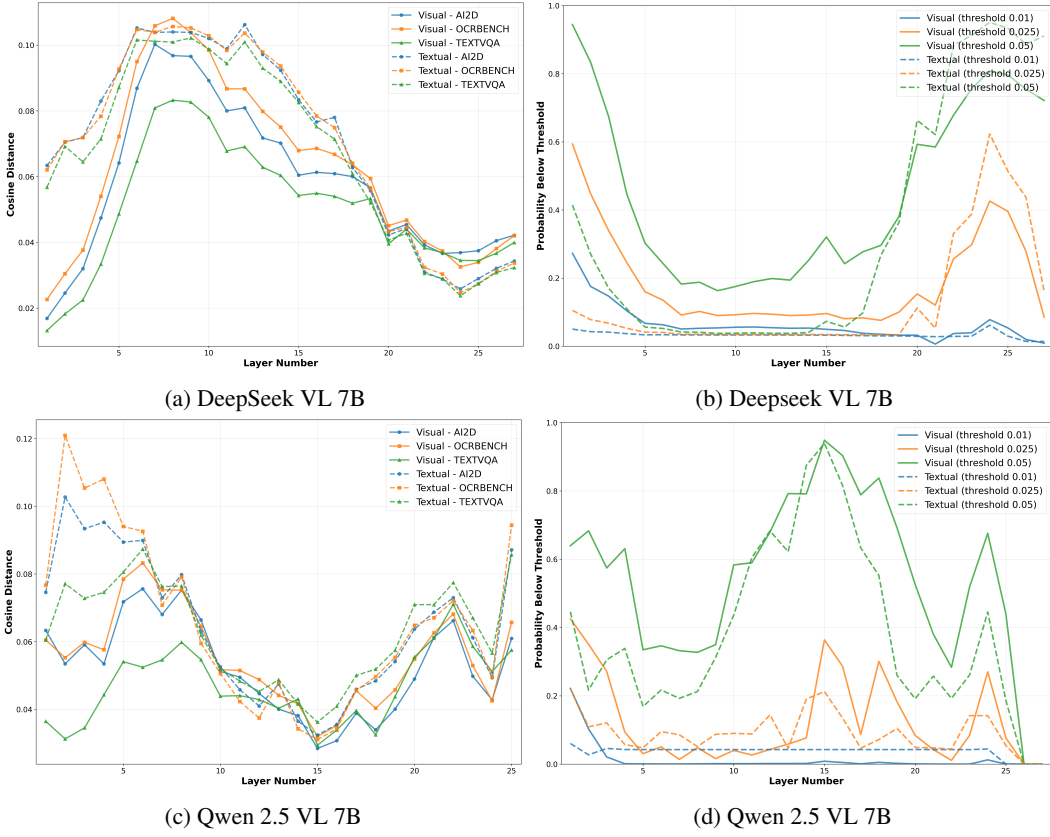


Figure 7: Empirical Geometric and Proximal Redundancy Experiments across layers for the Qwen 2.5 VL and Deepseek VL 7B VLMs. Across all datasets in the Text/Doc VQA task (see Table 3) and models, the early and late layer vision tokens have low adjacent token cosine distances.

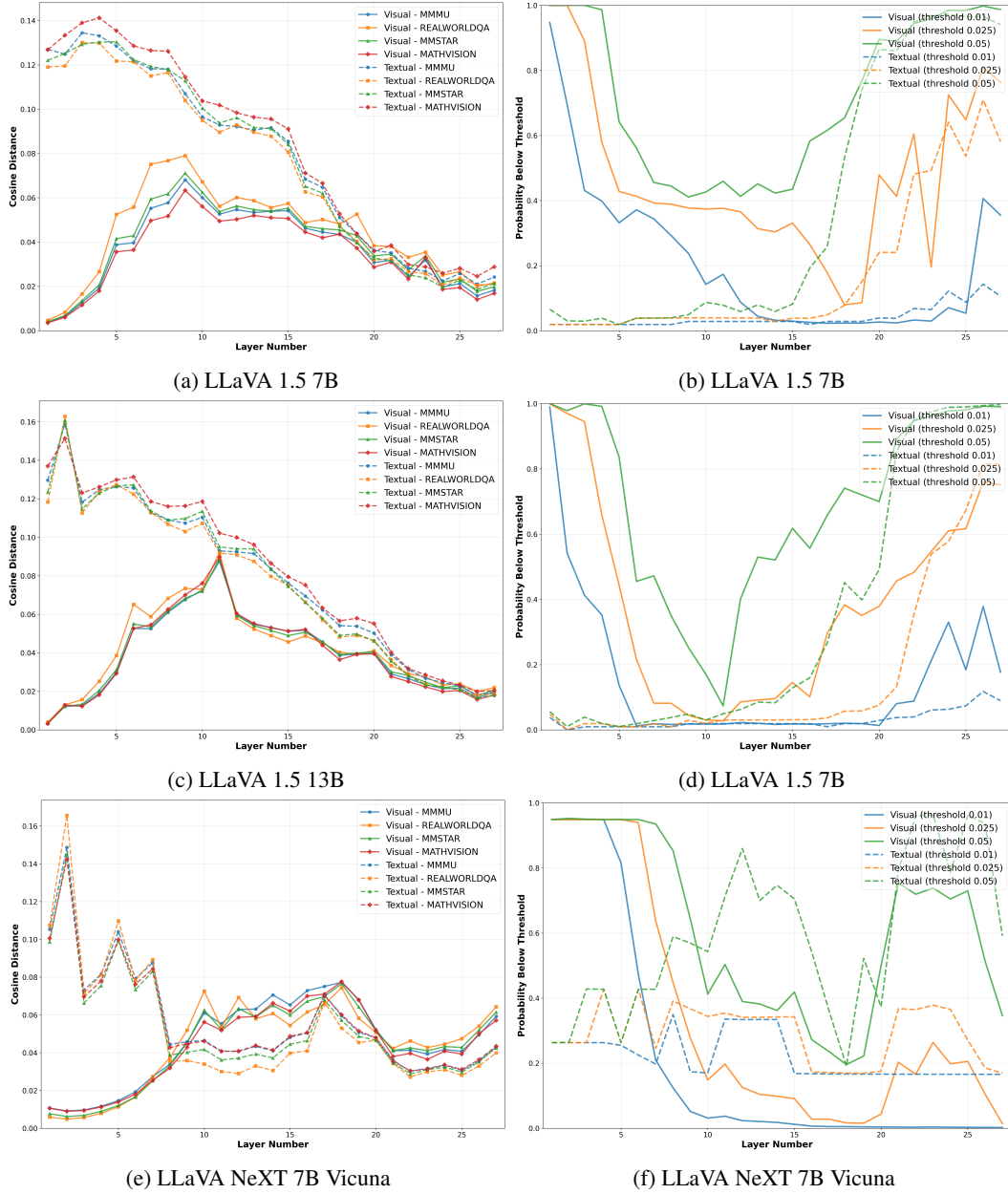


Figure 8: Empirical Geometric Redundancy between hidden states across layers for different VLMs. Across all the Multimodal Reasoning task (see Table 3) on the LLaVA, the early and late layer vision tokens have low adjacent token cosine distances.

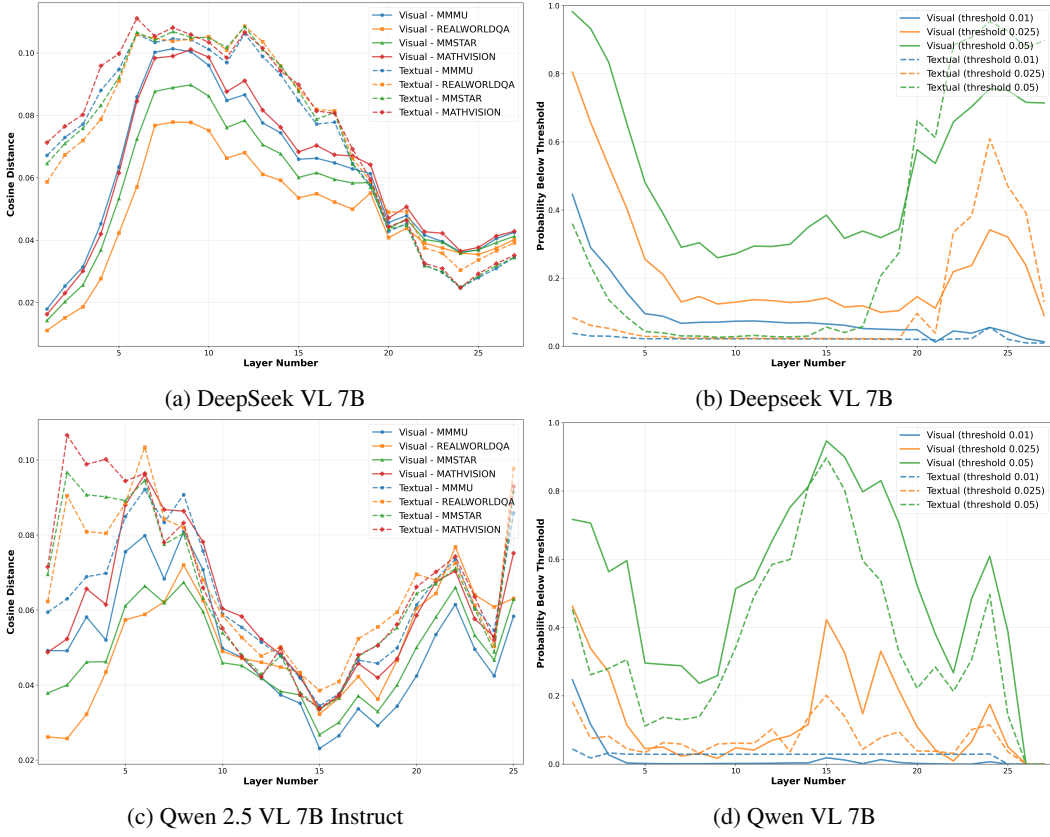


Figure 9: Empirical Geometric Redundancy between hidden states across layers for different VLMs. Across all the Multimodal Reasoning task (see Table 3) on Qwen 2.5 VL Instruct and DeepSeek VL 7B, the early and late layer vision tokens have low adjacent token cosine distances.

D FURTHER RESULTS FROM SECTION 5

In this section, we include plots of the skipping experiments for LLaVA 1.5 7B/13B and LLaVA NeXT 7B Vicuna on all datasets.

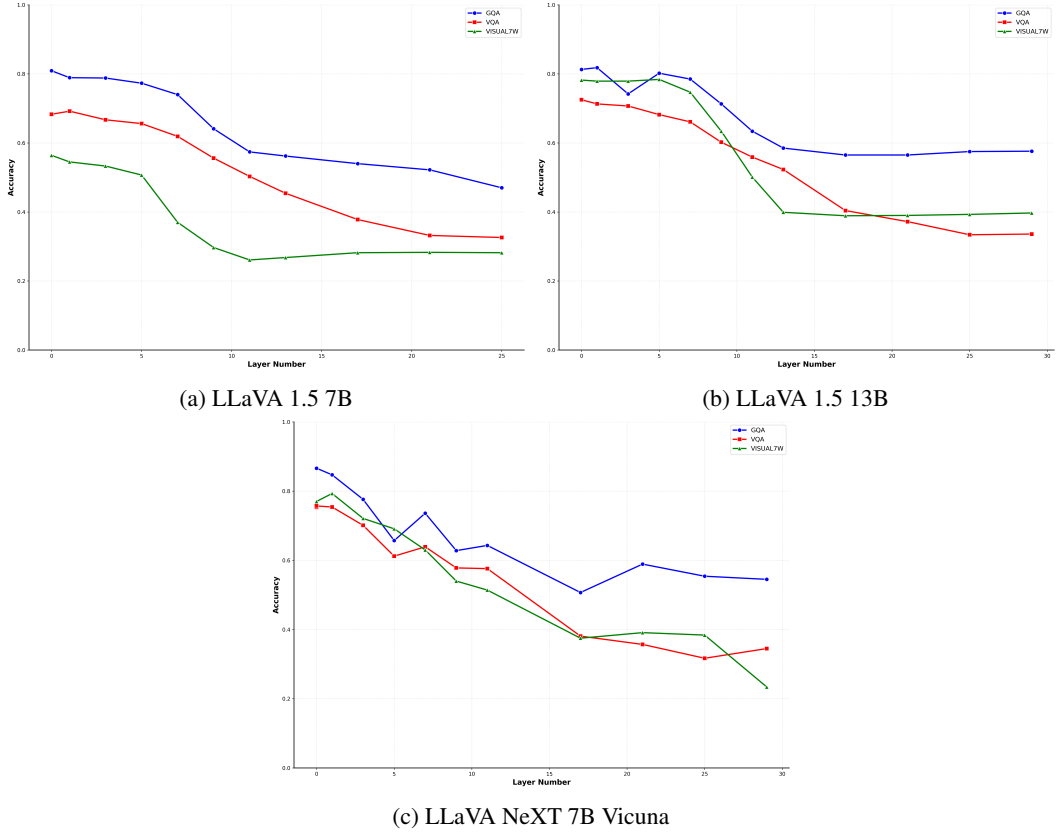


Figure 10: Skipping model accuracy versus layer. Run across all of the General VQA tasks (see Table 3) on the LLaVA models. The sharpest decrease in the early-middle layers.

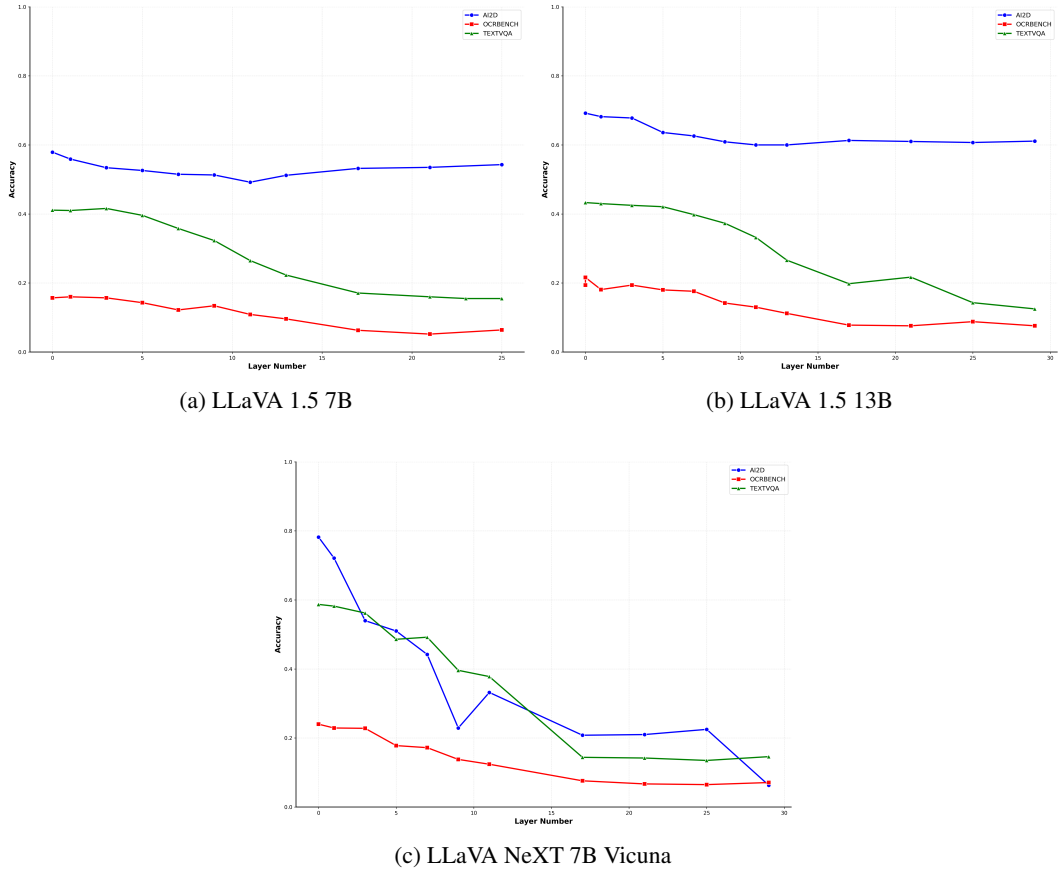


Figure 11: Skipping model accuracy versus layer. Run across all of the Text/Doc VQA tasks (see Table 3) on the LLaVA models. The sharpest decrease in the early-middle layers.

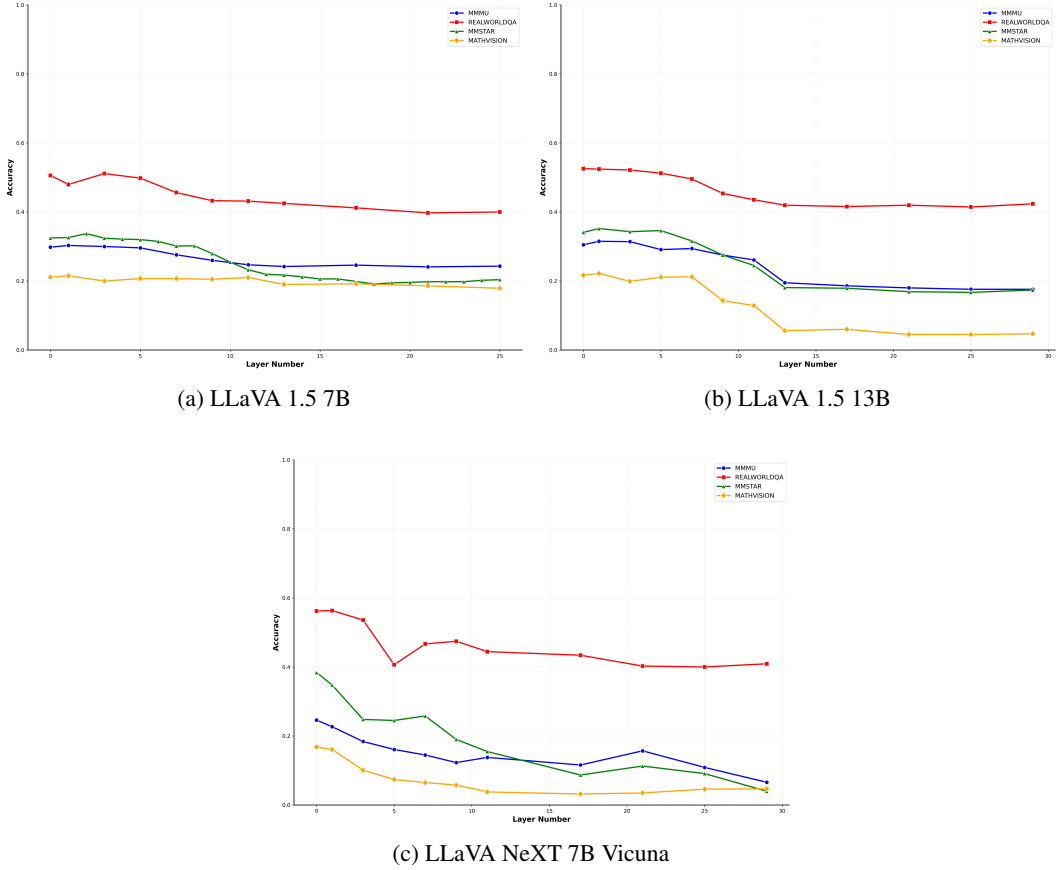


Figure 12: Skipping model accuracy versus layer. Run across all of the Multi-modal reasoning tasks (see Table 3) on the LLaVA models. The sharpest decrease in the early-middle layers.

E CONNECTION TO PID

For readers familiar with information theory, much of the vocabulary and intuition discussed regarding informational redundancy may sound very similar to notions of redundant and unique information in partial information decomposition (PID). PID (of 3 finite-support random variables) proposes that the mutual information $I(X; Y, Z)$ can be decomposed into the following terms.

1. Unique Information: $Uni(X : Y \setminus Z)$ and $Uni(X : Z \setminus Y)$ for the unique information that Y contains about X and Z contains about X respectively.
2. Redundant Information: $Red(X : Y, Z)$, which is the information about X that both Y and Z share.
3. Synergistic Information (sometimes called Shared Information): $Syn(X : Y, Z)$, which is the information about X that can only be derived from the combination of both Y and Z .

The proposed decomposition of the mutual information is given by the following definition.

Definition 5 (Partial Information Decomposition).

$$\begin{aligned}
 I(X; Y, Z) &\triangleq Uni(X : Y \setminus Z) + Uni(X : Z \setminus Y) + Red(X : Y, Z) + Syn(X : Y, Z) \\
 I(X; Y) &\triangleq Uni(X : Y \setminus Z) + Red(X : Y, Z) \\
 I(X; Z) &\triangleq Uni(X : Z \setminus Y) + Red(X : Y, Z).
 \end{aligned}$$

In fact, the connection between PID and informational redundancy can be somewhat formalized through the following observation.

Lemma 5. Let X, Y be discrete random variables. Then $\text{Uni}(X : X \setminus Y) = H(X|Y)$.

Proof. From the chain rule for mutual information we know that $I(X; Y|Z) = I(X; Y, Z) - I(X; Z)$. Using Definition 5 we see that $I(X; Y|Z) = \text{Uni}(X : Y \setminus Z) + \text{Syn}(X : Y, Z)$ and similarly, $I(X; Z|Y) = \text{Uni}(X : Z \setminus Y) + \text{Syn}(X : Y, Z)$. Thus $I(X; Y|X) = 0 = \text{Uni}(X : Y \setminus X) + \text{Syn}(X : X, Y)$. By the non-negativity of PID we get that $\text{Uni}(X : Y \setminus X) = \text{Syn}(X : X, Y) = 0$. Thus, $I(X; X|Y) = H(X|Y) = \text{Uni}(X : X \setminus Y)$. \square

Thus, if one considers $X = X_\ell, Y = X_{\ell-1}$, we recover our definition of informational redundancy using PID. This also offers a PID interpretation of redundancy: the unique information about the current layer, which only the current layer has, should be low. Further, since PID considers three random variables, this also allows us to consider a combination of our functional and informational redundancy by considering the quantity $\text{Uni}(Z : X_\ell \setminus X_{\ell-1})$. This would be the unique information that X_ℓ has about a target random variable Z that $X_{\ell-1}$ does not have.

The unique information quantity $\text{Uni}(X : Y \setminus Z)$ also has a widely accepted definition given by Bertschinger et al. (2014), which is the solution to following convex optimization problem:

Definition 6 (BROJA definition; (Bertschinger et al., 2014)).

$$\text{Uni}(X : Y \setminus Z) \triangleq \min_{Q \in \Delta_P} I_Q(X : Y|Z) \quad (33)$$

where Δ is the set of all joint distributions on X, Y, Z and $\Delta_P = \{Q \in \Delta : Q(X = x, Y = y) = P(X = x, Y = y) \text{ and } Q(X = x, Z = z) = P(X = x, Z = z) \forall x \in \text{supp}(X), y \in \text{supp}(Y), z \in \text{supp}(Z)\}$. That is the set of distributions that agree on the marginals.

If one can bound this value, then they recover a “functional information-theoretic redundancy”.